Sección: Revisiones y tutoriales / Section: Reviews and tutorials

Optical trapping: A review of essential concepts

Trampas ópticas: Revisión de conceptos esenciales

Ione Verdeny, Arnau Farré, Josep Mas, Carol López-Quesada,
Estela Martín-Badosa(†), Mario Montes-Usategui(*,†)

Optical Trapping Lab - Grup de Biofotònica (BiOPT), Departament de Física Aplicada i Òptica, Universitat de Barcelona, Martí i Franquès 1, 08028-Barcelona, Spain.

(*) Email: mario_montes@ub.edu (†) These authors equally contributed to this work

Recibido / Received: 15/04/2011. Revisado / Revised:08/06/2011. Aceptado / Accepted: 10/06/2011.

ABSTRACT:

Optical tweezers are an innovative technique for the non-contact, all-optical manipulation of small material samples, which has extraordinarily expanded and evolved since its inception in the mid-80s of the last century. Nowadays, the potential of optical tweezers has been clearly proven and a wide range of applications both from the physical and biological sciences have solidly emerged, turning the early ideas and techniques into a powerful paradigm for experimentation in the micro- and nanoworld. This review aims at highlighting the fundamental concepts that are essential for a thorough understanding of optical trapping, making emphasis on both its manipulation and measurement capabilities, as well as on the vast array of important biological applications appeared in the last years.

Keywords: Biophotonics, Radiation Pressure, Optical Trapping, Optical Tweezers, Optical Manipulation, Holographic Optical Elements, Spatial Light Modulators.

RESUMEN:

Las pinzas ópticas constituyen una técnica innovadora para la manipulación óptica no invasiva de pequeñas muestras materiales, que desde su comienzo a mediados de los años 80 del siglo pasado ha evolucionado y se ha extendido de manera extraordinaria. En la actualidad, el potencial de las pinzas ópticas ha sido claramente demostrado y han surgido con fuerza un amplio rango de aplicaciones, tanto en el campo de la física como en el de la biología, que han convertido las primeras ideas y técnicas en un potente paradigma para la experimentación en el mundo micro- y nanométrico. Este artículo de revisión pretende poner de relieve aquellos conceptos fundamentales que son esenciales para entender las pinzas ópticas en profundidad, haciendo énfasis tanto en su capacidad de manipulación como de medida, así como en el inmenso conjunto de aplicaciones biológicas que han aparecido en los últimos años.

Palabras clave: Biofotónica, Presión de Radiación, Trampas Ópticas, Pinzas Ópticas, Manipulación Óptica, Elementos Ópticos Holográficos, Moduladores Espaciales de Luz.

REFERENCES AND LINKS

[1]. A. Ashkin, "Acceleration and trapping of particles by radiation pressure", *Phys. Rev. Lett.* **24**, 156–159 (1970).

[2]. S. M. Block, L. S. Goldstein, B. J. Schnapp, "Bead movement by single kinesin molecules studied with optical tweezers", *Nature* **348**, 348–352 (1990).

[3]. C. Shingyoji, H. Higuchi, M. Yoshimura, E. Katayama, T. Yanagida, "Dynein arms are oscillating force generators", *Nature* **393**, 711–714 (1998).

[4]. J. T. Finer, R. M. Simmons, J. A. Spudich, "Single myosin molecule mechanics: piconewton forces and nanometre steps", *Nature* **368**, 113–119 (1994).

[5]. H. Yin, M. D. Wang, K. Svoboda, R. Landick, S. M. Block, J. Gelles, "Transcription against an applied force", *Science* **270**, 1653–1657 (1995).

[6]. M. S. Z. Kellermayer, S. B. Smith, H. L. Granzier, C. Bustamante, "Folding-unfolding transitions in single titin molecules characterized with laser tweezers", *Science* **276**, 1112–1116 (1997).

[7]. O. Thoumine, P. Kocian, A. Kottelat, J. J. Meister, "Short-term binding of fibroblasts to fibronectin: optical tweezers experiments and probabilistic analysis", *Eur. Biophys. J.* **29**, 398-408 (2000).

[8]. S. J. Kotch, A. Shundrovsky, B. C. Jantzen, M. D. Wang, "Probing protein-DNA interactions by unzipping a single DNA double helix", *Biophys. J.* **83**, 1098–1105 (2002).

[9]. S. B. Smith, Y. Cui, C. Bustamante, "Overstretching B-DNA: the elastic response of individual doublestranded and single-stranded DNA molecules", *Science* **271**, 795–799 (1996).

[10]. E. Townes-Anderson, R. S. St Jules, D. M. Sherry, J. Lichtenberger, M. Hassanain, "Micromanipulation of retinal neurons by optical tweezers", *Mol. Vis.* **4**, 12 (1998).

[11]. M. W. Berns, Y. Tadir, H. Liang, B. Tromberg, "Laser scissors and tweezers", *Method. Cell Biol.* **55**, 71–98 (1998).

[12]. A. Ehrlicher, T. Betz, B. Stuhrmann, D. Koch, V. Milner, M. G. Raizen, J. Kas, "Guiding neuronal growth with light", *P. Natl. Acad. Sci. USA.* **99**, 16024–16028 (2002).

[13]. J. Guck, R. Ananthakrishnan, H. Mahmood, T. J. Moon, C. C. Cunningham, J. Käs, "The optical stretcher: a novel laser tool to micromanipulate cells", *Biophys. J.* **81**, 767–784 (2001).

[14]. S. P. Gross, M. A. Welte, S. M. Block, E. F. Wieschaus, "Dynein-mediated cargo transport in vivo. A switch controls travel distance", *J. Cell Biol.* **148**, 945–956 (2000).

[15]. J. E. Curtis, B. A. Koss, D. G. Grier, "Dynamic holographic optical tweezers", *Opt. Commun.* **207**, 169-175 (2002).

[16]. P. T. Korda, M. B. Taylor, D. G. Grier, "Kinetically locked-in colloidal transport in an array of optical tweezers", *Phys. Rev. Lett.* **89**, 128301 (2002).

[17]. D. R. Burnham, D. McGloin, "Holographic optical trapping of aerosol droplets", *Opt. Express* **14**, 4176-4182 (2006).

[18]. J. Plewa, E. Tanner, D. M. Mueth, D. G. Grier, "Processing carbon nanotubes with holographic optical tweezers", *Opt. Express* **12**, 1978-1981 (2004).

[19]. P. J. Pauzauskie, A. Radenovic, E. Trepagnier, H. Shroff, P. Yang, J. Liphardt, "Optical trapping and integration of semiconductor nanowire assemblies in water", *Nat. Mater.* **5**, 97–101 (2006).

[20]. K. C. Neuman, S. M. Block, "Optical trapping", *Rev. Sci. Instrum.* **75**, 2787–2809 (2004).

[21]. K. Dholakia, P. Reece, "Optical micromanipulation takes hold", *Nano Today* **1**, 1-27 (2006).

[22]. H. Zhang, K.-K. Liu, "Optical tweezers for single cells", *J. R. Soc. Interface* **5**, 671-690 (2008).

[23]. J. R. Moffitt, Y. R. Chemla, S. B. Smith, C. Bustamante, "Recent advances in optical tweezers", *Annu. Rev. Biochem.* **77**, 205–228 (2008).

[24]. K. Ramser, D. Hanstorp, "Optical manipulation for single-cell studies", *J. Biophotonics* **3**, 187-206 (2010).

[25]. D. J. Stevenson, F. Gunn-Moore, K. Dholakia, "Light forces the pace: optical manipulation for biophotonics", *J. Biomed. Opt.* **15**, 041503 (2010).

[26]. D. G. Grier, "A revolution in optical manipulation", *Nature* **424**, 810–816 (2003).

[27]. K. Dholakia, P. Reece, M. Gu, "Optical micromanipulation", *Chem. Soc. Rev.* **37**, 42-55 (2008).

[28]. S. Hormeño, J. R. Arias-González, "Exploring mechanochemical processes in the cell with optical tweezers", *Biol. Cell* **98**, 679-695 (2006).

[29]. A. Ashkin, J. Dziedzic, J. E. Bjorkholm, S. Chu, "Observation of a single-beam gradient force optical trap for dielectric particles", *Opt. Lett.* **11**, 288–290 (1986).

[30]. J. P. Gordon, A. Ashkin, "Motion of atoms in a radiation trap", *Phys. Rev. A* **21**, 1606-1617 (1980).

[31]. J. Mas, A. Farré, J. Cuadros, I. Juvells, A. Carnicer, "Understanding optical trapping phenomena: A simulation for undergraduates", *IEEE T. Educ.* **54**, 133-140 (2011).

[32]. R. N. C. Pfeifer, T. A. Nieminen, N. R. Heckenberg, H. Rubinsztein-Dunlop, "Two controversies in classical electromagnetism", *Proc. SPIE* **6326**, 63260H (2006).

[33]. P. C. Chaumet, "Comment on 'Trapping force, force constant, and potential depths for dielectric spheres in the presence of spherical aberrations'", *Appl. Opt.* **43**, 1825-1826 (2004).

[34]. T. A. Nieminen, V. L. Y. Loke, A. B. Stilgoe, G. Knöner, A. M. Branczyk, N. R. Heckenberg, H. Rubinsztein-Dunlop, "Optical tweezers computational toolbox", *J. Opt. A* **9**, S196–S203 (2007).

[35]. G. Gouesbet, "Generalized Lorentz-Mie theory and applications", *Part. Part. Syst. Charact.* **11**, 22–34 (1994).

[36]. Y. Harada, T. Asakura, "Radiation forces on a dielectric sphere in the Rayleigh scattering regime", *Opt. Commun.* **124**, 529–541 (1996).

[37]. A. Ashkin, "Forces of a single-beam gradient laser trap on a dielectric sphere in the ray optics regime", *Biophys. J.* **61**, 569–582 (1992).

[38]. F. Gittes, C. F. Schmidt, "Interference model for back-focal-plane displacement detection in optical tweezers", *Opt. Lett.* **23**, 7–9 (1998).

[39]. W. H. Wright, G. J. Sonek, "Radiation trapping forces on microspheres with optical tweezers", *Appl. Phys. Lett.* **63**, 715-717 (1993).

[40]. C. M. Creely, G. Volpe, G. P. Singh, M. Soler, D. V. Petrov, "Raman imaging of floating cells", *Opt. Express* **13**, 6105–6110 (2005).

[41]. E. A. Abbondanzieri, W. J. Greenleaf, J. W. Shaevitz, R. Landick, S. M. Block, "Direct observation of base-pair stepping by RNA polymerase", *Nature* **438**, 460–465 (2005).

[42]. M. C. Noom, B. van den Broek, J. van Mameren, G. J. L. Wuite, "Visualizing single DNA-bound proteins using DNA as a scanning probe", *Nature Meth.* **4**, 1031-1036 (2007).

[43]. E. Pleguezuelos, A. Carnicer, J. Andilla, E. Martín-Badosa, M. Montes-Usategui, "HoloTrap: Interactive hologram design for multiple dynamic optical trapping", *Comp. Phys. Commun.* **176**, 701-709 (2007).

[44]. K. Visscher, S. P. Gross, S. M. Block, "Construction of multiple-beam optical traps with nanometer resolution position sensing", *IEEE J. Sel. Top. Quantum Electron.* **2**, 1066–1076 (1996).

[45]. W. H. Guilford, J. A. Tournas, D. Dascalu, D. S. Watson, "Creating multiple time-shared laser traps with simultaneous displacement detection using digital signal processing hardware", *Anal. Biochem.* **326**, 153-166 (2004).

[46]. Y. Hayasaki, M. Itoh, T. Yatagai, N. Nishida, "Nonmechanical optical manipulation of microparticle using spatial light modulator", *Opt. Rev.* **6**, 24–27 (1999).

[47]. R. W. Gerchberg, W. O. Saxton, "A practical algorithm for the determination of phase from image and diffraction plane pictures", *Optik* **35**, 237–246 (1971).

[48]. J. Liesener, M. Reicherter, T. Haist, H. Tiziani, "Multi-functional optical tweezers using computer-generated holograms", *Opt. Commun.* **185**, 77–82 (2000).

[49]. G. M. Gibson, J. Leach, S. Keen, A. J. Wright, M. J. Padgett, "Measuring the accuracy of particle position and force in optical tweezers using high-speed video microscopy", *Opt. Express* **16**, 14561-14570 (2008).

[50]. R. W. Bowman, A. J. Wright, M. J. Padgett, "An SLM-based Shack-Hartmann wavefront sensor for aberration correction in optical tweezers", *J. Opt.* **12**, 124004 (2010).

[51]. A. Jesacher, A. Schwaighofer, S. Fürhapter, C. Maurer, S. Bernet, M. Ritsch-Marte, "Wavefront correction of spatial light modulators using an optical vortex image", *Opt. Express* **15**, 5801-5808 (2007).

[52]. C. López-Quesada, J. Andilla, E. Martín-Badosa, "Correction of aberration in holographic optical tweezers using a Shack-Hartmann sensor", *Appl. Opt.* **48**, 1084-1090 (2009).

[53]. S. Zwick, T. Haist, Y. Miyamoto, L. He, M. Warber, A. Hermerschmidt, W. Osten, "Holographic twin traps", *J. Opt. A-Pure Appl. Opt.* **11**, 034011 (2009).

[54]. J. A. Grieve, A. Ulcinas, S. Subramanian, G. M. Gibson, M. J. Padgett, D. M. Carberry, M. J. Miles, "Hands-on with optical tweezers: a multitouch interface for holographic optical trapping", *Opt. Express* **17**, 3595-3602 (2009).

[55]. A. van der Horst, N. R. Forde, "Calibration of dynamic holographic optical tweezers for force measurements on biomaterials", *Opt. Express* **16**, 20987-21003 (2008).

[56]. A. Lizana, A. Márquez, L. Lobato, Y. Rodange, I. Moreno, C. Iemmi, J. Campos, "The minimum Euclidean distance principle applied to improve the modulation diffraction efficiency in digitally controlled spatial light modulators", *Opt. Express* **18**, 10581-10593 (2010).

[57]. W. Denk, W. W. Webb, "Optical measurement of picometer displacements of transparent microscopic objects", *Appl. Opt.* **29**, 2382–2391 (1990).

[58]. K. Svoboda, C. F. Schmidt, B. J. Schnapp, S. M. Block, "Direct observation of kinesin stepping by optical trapping interferometry", *Nature* **365**, 721–727 (1993).

[59]. L. P. Ghislain, W. W. Webb, "Scanning-force microscope based on an optical trap", *Opt. Lett.* **18**, 1678–1680 (1993).

[60]. L. P. Ghislain, N. A. Switz, W. W. Webb, "Measurement of small forces using an optical trap", *Rev. Sci. Instrum.* **65**, 2762–2768 (1994).

[61]. J. E. Molloy, J. E. Burns, J. Kendrick-Jones, R. T. Tregear, D. C. White, "Movement and force produced by a single myosin head", *Nature* **378**, 209–212 (1995).

[62]. M. Capitanio, D. Maggi, F. Vanzi, F. S. Pavone, "FIONA in the trap: the advantages of combining optical tweezers and fluorescence", *J. Opt. A-Pure Appl. Opt.* **9**, S157–S163 (2007).

[63]. M. W. Allersma, F. Gittes, M. J. deCastro, R. J. Stewart, C. F. Schmidt, "Two-dimensional tracking of ncd motility by back focal plane interferometry", *Biophys. J.* **74**, 1074–1085 (1998).

[64]. M. J. Lang, C. L. Asbury, J. W. Shaevitz, S. M. Block, "An automated two-dimensional optical force clamp for single molecule studies", *Biophys. J.* **83**, 491–501 (2002).

[65]. A. Rohrbach, E. H. K. Stelzer, "Three-dimensional position detection of optically trapped dielectric particles", *J. Appl. Phys.* **91**, 5474–5488 (2002).

[66]. K. Berg-Sorensen, H. Flyvbjerg, "Power spectrum analysis for optical tweezers", *Rev. Sci. Instrum.* **75**, 594–612 (2004).

[67]. M. Capitanio, G. Romano, R. Ballerini, M. Giuntini, F. S. Pavone, "Calibration of optical tweezers with differential interference contrast signals", *Rev. Sci. Instrum.* **73**, 1687-1696 (2002).

[68]. S. C. Kuo, M. P. Sheetz, "Force of single kinesin molecules measured with optical tweezers", *Science* **260**, 232–243 (1993).

[69]. R. M. Simmons, J. T. Finer, S. Chu, J. A. Spudich, "Quantitative measurements of force and displacement using an optical trap", *Biophys. J.* **70**, 1813–1822 (1996).

[70]. M. D. Wang, H. Yin, R. Landick, J. Gelles, S. M. Block, "Stretching DNA with optical tweezers", *Biophys. J.* **72**, 1335–1346 (1997).

[71]. E.-L. Florin, A. Pralle, E. H. K. Stelzer, J. K. H. Hörber, "Photonic force microscope calibration by thermal noise analysis", *Appl. Phys., A Mater. Sci. Process.* **66**, S75–S78 (1998).

[72]. I. M. Tolic-Norrelykke, K. Berg-Sorensen, H. Flyvbjerg, "MatLab program for precision calibration of optical tweezers", *Comput. Phys. Commun.* **159**, 225-240 (2004).

[73]. E. J. G. Peterman, F. Gittes, C. F. Schmidt, "Laser-induced heating in optical traps", *Biophys. J.* **84**, 1308-1316 (2003).

[74]. A. C. Richardson, S. N. S. Reihani, L. B. Oddershede, "Non-harmonic potential of a single beam optical trap", *Opt. Express* **16**, 15709-15717 (2008).

[75]. S. F. Tolic-Norrelykke, E. Schäffer, J. Howard, F. S. Pavone, F. Jülicher, H. Flyvbjerg, "Calibration of optical tweezers with positional detection in the back focal plane", *Rev. Sci. Instrum.* **77**, 103101 (2006).

[76]. S. C. Kuo, J. L. McGrath, "Steps and fluctuations of Listeria monocytogenes during actin-based motility", *Nature* **407**, 1026–1029 (2000).

[77]. P. C. Seitz, E. H. K. Stelzer, A. Rohrbach, "Interferometric tracking of optically trapped probes behind structured surfaces: A phase correction method", *Appl. Opt.* **45**, 7309–7315 (2006).

[78]. S. B. Smith, Y. Cui, C. Bustamante, "Optical-trap force transducer that operates by direct measurement of light momentum", *Methods Enzymol.* **361**, 134–162 (2003).

[79]. A. Farré, M. Montes-Usategui, "A force detection technique for single-beam optical traps based on direct measurement of light momentum changes", *Opt. Express* **18**, 11955-11967 (2010).

[80]. A. Ashkin, J. M. Dziedzic, "Optical trapping and manipulation of viruses and bacteria", *Science* **235**, 1517-1520 (1987).

[81]. http://www.bell-labs.com/user/feature/archives/ashkin/

[82]. A. Farré, C. López-Quesada, J. Andilla, E. Martín-Badosa, M. Montes-Usategi, "Holographic optical manipulation of motor-driven membranous structures in living NG-108 cells", *Opt. Eng.* **49**, 085801 (2010).

[83]. M. Torrent, B. Llompart, S. Lasserre-Ramassamy, I. Llop-Tous, M. Bastida, P. Marzabal, A. Westerholm-Pavinen, M. Saloheimo, P. B. Heifetz, M. D. Ludevid, "Eukaryotic protein production in designed storage organelles", *BMC Biology* 7:5 (2009).

[84]. K. Svoboda, S.M. Block, "Force and velocity measured for single kinesin molecules", *Cell* **77**, 773–784 (1994).

[85]. S. M. Block, "Kinesin motor mechanics: binding, stepping, tracking, gating, and limping", *Biophys. J.* 92, 2986–2995 (2007).

[86]. A. Gennerich, A. P. Carter, S. L. Reck-Peterson, R. D. Vale, "Force-induced bidirectional stepping of cytoplasmic dynein", *Cell* **131**, 952–965 (2007).

[87]. P. A. Sims, X. S. Xie, "Probing dynein and kinesin stepping with mechanical manipulation in a living cell", *ChemPhysChem* **10**, 1511–1516 (2009).

[88]. C. Kural, A. S. Serpinskaya, Y.-H. Chou, R. D. Goldman, V. I. Gelfand, P. R. Selvin, "Tracking melanosomes inside a cell to study molecular motors and their interaction", *P. Natl. Acad. Sci. USA* **104**, 5378-5382 (2007).

[89]. X. Nan, P. A. Sims, X. S. Xie, "Organelle tracking in a living cell with microsecond time resolution and nanometer spatial precision", *ChemPhysChem* **9**, 707-712 (2008).

[90]. P. Pierobon, S. Achouri, S. Courty, A. R. Dunn, J. A. Spudich, M. Dahan, G. Cappello, "Velocity, processivity and individual steps of single Myosin V molecules in live cells", *Biophys. J.* **96**, 4268-4275 (2009).

[91]. M. D. Wang, M. J. Schnitzer, H. Yin, R. Landick, J. Gelles, S. M. Block, "Force and velocity measured for single molecules of RNA polymerase", *Science* **282**, 902–907 (1998).

[92]. G. J. L. Wuite, S. B. Smith, M. Young, D. Keller, C. Bustamante, "Single-molecule studies of the effect of template tension on T7 DNA polymerase activity", *Nature* **404**, 103–106 (2000).

[93]. T. T. Perkins, H.-W. Li, R. V. Dalal, J. Gelles, S. M. Block, "Forward and reverse motion of single RecBCD molecules on DNA", *Biophys. J.* **86**, 1640–1648 (2004).

[94]. S. Dumont, W. Cheng, V. Serebrov, R. K. Beran, I. Jr. Tinoco, A. M. Pyle, C. Bustamante, "RNA translocation and unwinding mechanism of HCV NS3 helicase and its coordination by ATP", *Nature* **439**, 105–108 (2006).

[95]. M. D. Stone, Z. Bryant, N. J. Crisona, S. B. Smith, A. Vologodskii, C. Bustamante, N. R. Cozzarelli, "Chirality sensing by Escherichia coli topoisomerase IV and the mechanism of type II topoisomerases", *P. Natl. Acad. Sci. USA* **100**, 8654–8659 (2003).

[96]. T. T. Perkins, R. V. Dalal, P. G. Mitsis, S. M. Block, "Sequence-dependent pausing of single lambda exonuclease molecules", *Science* **301**, 1914–1918 (2003).

[97]. P. J. Pease, O. Levy, G. J. Cost, J. Gore, J. L. Ptacin, D. Sherratt, C. Bustamante, N. R. Cozzarelli, "Sequence-directed DNA translocation by purified FtsK", *Science* **307**, 586–590 (2005).

[98]. D. E. Smith, S. J. Tans, S. B. Smith, S. Grimes, D. L. Anderson, C. Bustamante, "The bacteriophage straight ϕ29 portal motor can package DNA against a large internal force", *Nature* **413**, 748–752 (2001).

[99]. Y. R. Chemla, K. Aathavan, J. Michaelis, S. Grimes, P. J. Jardine, D. L. Anderson, C. Bustamante, "Mechanism of force generation of a viral DNA packaging motor", *Cell* **122**, 683–692 (2005).

[100]. W. S. Ryu, R. M. Berry, H. C. Berg, "Torque-generating units of the flagellar motor of Escherichia coli have a high duty ratio", *Nature* **403**, 444-447 (2000).

[101]. J. M. Nascimento, E. L. Botvinick, L. Z. Shi, B. Durrant, M. W. Berns, "Analysis of sperm motility using optical tweezers", *J. Biomed. Opt.* **11**, 044001(2006).

[102]. J. D. Wen, L. Lancaster, C. Hodges, A. C. Zeri, S. H. Yoshimura, H. F. Noller, C. Bustamante, I. Tinoco, "Following translation by single ribosomes one codon at a time", *Nature* **452**, 598–603 (2008).

[103]. Y. Tsuda, H. Yasutake, A. Ishijima, T. Yanagida, "Torsional rigidity of single actin filaments and actin-actin bond breaking force under torsion measured directly by in vitro micromanipulation", *P. Natl. Acad. Sci. USA* **93**, 12937–12942 (1996).

[104]. Y. Arai, K. Akashi, Y. Harada, H. Miyata, K. Kinosita Jr., H. Itoh, "Tying a molecular knot with optical tweezers", *Nature* **399**, 446-449 (1999).

[105]. M. Kurachi, M. Hoshi, H. Tashiro, "Buckling of a single microtubule by optical trapping forces: direct measurement of microtubule rigidity", *Cell Motil. Cytoskel.* **30**, 221–228 (1995).

[106]. H. Felgner, R. Frank, M. Schliwa, "Flexural rigidity of microtubules measured with the use of optical tweezers", *J. Cell Sci.* **109**, 509-516 (1996).

[107]. J. M. Huguet, C. V. Bizarro, N. Forns, S. B. Smith, C. Bustamante, F. Ritort, "Single-molecule derivation of salt dependent base-pair free energies in DNA", *P. Natl. Acad. Sci. USA* **107**, 15431–15436 (2010).

[108]. J. Liphardt, B. Onoa, S. B. Smith, I. J. Tinoco, C. Bustamante, "Reversible unfolding of single RNA molecules by mechanical force", *Science* **292**, 733–737 (2001).

[109]. C. Bustamante, Z. Bryant, S. B. Smith, "Ten years of tension: single-molecule DNA mechanics", *Nature* **421**, 423-427 (2003).

[110]. L. Tskhovrebova, J. Trinick, J. A. Sleep, R. M. Simmons, "Elasticity and unfolding of single molecules of the giant muscle protein titin", *Nature* **387**, 308–312 (1997).

[111]. C. Cecconi, E. A. Shank, C. Bustamante, S. Marqusee, "Direct observation of the three-state folding of a single protein molecule", *Science* **309**, 2057–2060 (2005).

[112]. M. C. Williams, I. Rouzina, J. R. Wenner, R. J. Gorelick, K. Musier-Forsyth, V. A. Bloomfield, "Mechanism for nucleic acid chaperone activity of HIV-1 nucleocapsid protein revealed by single molecule stretching", *P. Natl. Acad. Sci. USA* **98**, 6121-6126 (2001).

[113]. Y. Cui, C. Bustamante, "Pulling a single chromatin fiber reveals the forces that maintain its higher-order structure", *P. Natl. Acad. Sci. USA* **97**, 127–132 (2000).

[114]. M. L. Bennink, S. H. Leuba, G. H. Leno, J. Zlatanova, B. G. de Grooth, J. Greve, "Unfolding individual nucleosomes by stretching single chromatin fibers with optical tweezers", *Nat. Struct. Biol.* **8**, 606–610 (2001).

[115]. B. D. Brower-Toland, C. L. Smith, R. C. Yeh, J. T. Lis, C. L. Peterson, M. D. Wang, "Mechanical disruption of individual nucleosomes reveals a reversible multistage release of DNA", *P. Natl. Acad. Sci. USA* **99**, 1960–1965 (2002).

[116]. J. Enger, M. Goksör, K. Ramser, P. Hagberg, D. Hanstorp, "Optical tweezers applied to a microfluidic system", *Lab Chip* **4**, 196-200 (2004).

[117]. E. Eriksson, J. Enger, B. Nordlander, N. Erjavec, K. Ramser, M. Goksor, S. Hohmann, T. Nystrom, D. Hanstorp, "A microfluidic system in combination with optical tweezers for analyzing rapid and reversible cytological alterations in single cells upon environmental changes", *Lab Chip* **7**, 71–76 (2006).

[118]. K. Ramser, J. Enger, M. Goksör, D. Hanstorp, K. Logg, M. Käll, "A microfluidic system enabling Raman measurements of the oxygenation cycle in single optically trapped red blood cells", *Lab Chip* **5**, 431-436 (2005).

[119]. G. P. Singh, C. Creely, G. Volpe, H. Groetsch, D. V. Petrov, "Real-time detection of hyperosmotic stress response in optically trapped single yeast cells using Raman miscrospectroscopy", *Anal. Chem.* **77**, 2564-2568 (2005).

[120]. Y. Wakamoto, I. Inoue, H. Moriguchi, K. Yasuda, "Analysis of single-cell differences by use of an on-chip microculture system and optical trapping", *Fresen. J. Anal. Chem.* **371**, 276-281 (2001).

[121]. D. Watson, N. Hagen, J. Diver, P. Marchand, M. Chachisvilis, "Elastic light scattering from single cells: Orientational dynamics in optical trap", *Biophys. J.* **87**, 1298–1306 (2004).

[122]. C. Xie, J. Mace, M. A. Dinno, Y. Q. Li, W. Tang, R. J. Newton, P. J. Gemperline, "Identification of single bacterial cells in aqueous solution using confocal laser tweezers Raman spectroscopy", *Anal. Chem.* **77**, 4390-4397 (2006).

[123]. J. W. Chan, D. S. Taylor, T. Zwerdling, S. M. Lane, K. Ihara, T. Huser, "Micro-Raman spectroscopy detects individual neoplastic and normal hematopoietic cells", *Biophys. J.* **90**, 648–656 (2006).

[124]. M. M. Wang, E. Tu, D. E. Raymond, J. M. Yang, H. Zhang, N. Hagen, B. Dees, E. M. Mercer, A. H. Forster, I. Kariv, P. J. Marchand, W. F. Butler, "Microfluidic sorting of mammalian cells by optical force switching", *Nat. Biotech.* 23, 83–87 (2005).

[125]. M. Ericsson, D. Hanstorp, P. Hagberg, J. Enger, T. Nystrom, "Sorting out bacterial viability with optical tweezers", *J. Bacteriol.* **182**, 5551–5555 (2000).

[126]. D. J. Odde, M. J. Renn, "Laser-guided direct writing of living cells", *Biotechnol. Bioeng.* **67**, 312–318 (2000).

[127]. J. Pine, G. Chow, "Moving live dissociated neurons with an optical tweezer", *IEEE Trans. Biomed. Eng.* **56**, 1184–1188 (2009).

[128]. C. Luo, H. Li, C. Xiong, X. Peng, Q. Kou, Y. Chen, H. Ji, Q. Ouyang, "The combination of optical tweezers and microwell array for cells physical manipulation and localization in microfluidic device", *Biomed. Microdevices* **9**, 573–578 (2007).

[129]. M. Ozkan, M. Wang, C. Ozkan, R. Flynn, A. Birkbeck, S. Esener, "Optical manipulation of objects and biological cells in microfluidic devices", *Biomed. Microdevices* **5**, 61–67 (2003).

[130]. M. Ozkan, T. Pisanic, J. Scheel, C. Barlow, S. Esener, S. N. Bhatia, "Electro-optical platform for the manipulation of live cells", *Langmuir* **19**, 1532–1538 (2003).

[131]. G. M. Akselrod, W. Timp, U. Mirsaidov, Q. Zhao, C. Li, R. Timp, K. Timp, P. Matsudaira, G. Timp, "Laser-guided assembly of heterotypic three-dimensional living cell microarrays", *Biophys. J.* **91**, 3465–3473 (2006).

[132]. M. He, J. S. Edgar, G. D. M. Jeffries, R. M. Lorenz, J. P. Shelby, D. T. Chiu, "Selective encapsulation of single cells and subcellular organelles into picoliter- and femtoliter-volume droplets", *Anal. Chem.* **77**, 1539–1544 (2005).

[133]. S. Seeger, S. Monajembashi, K. J. Hutter, G. Futterman, J. Wolfrum, K. O. Greulich, "Application of laser optical tweezers in immunology and molecular genetics", *Cytometry* **12**, 497–504 (1991).

[134]. H. Liang, W. H. Wright, C. L. Rieder, E. D. Salmon, G. Profeta, J. Andrews, Y. Liu, G. J. Sonek, M. W. Berns, "Directed movement of chromosome arms and fragments in mitotic newt lung cells using optical scissors and optical tweezers", *Exp. Cell Res.* **213**, 308–312 (1994).

[135]. N. Ponelies, J. Scheef, A. Harim, G. Leitz, K. O. Greulich, "Laser micromanipulators for biotechnology and genome research", *J. Biotechnol.* **35**, 109–120 (1994).

[136]. S. Kumar, I. Z. Maxwell, A. Heisterkamp, T. R. Polte, T. P. Lele, M. Salanga, E. Mazur, D. E. Ingber, "Viscoelastic retraction of single living stress fibers and its impact on cell shape, cytoskeletal organization, and extracellular matrix mechanics", *Biophys. J.* **90**, 3762–3773 (2006).

[137]. P. M. Lanigan, K. Chan, T. Ninkovic, R. H. Templer, P. M. French, A. J. de Mello, K. R. Willison, P. J. Parker, M. A. Neil, O. Ces, D. R. Klug, "Spatially selective sampling of single cells using optically trapped fusogenic emulsion droplets: a new single-cell proteomic tool", *J. R. Soc. Interface* **5**, S161–S168 (2008).

[138]. G. Leitz, C. Lundberg, E. Fällman, O. Axner, A. Sellstedt, "Laser-based micromanipulation for separation and identification of individual Frankia vesicles", *FEMS Microbiol. Lett.* **224**, 97–100 (2003).

[139]. R. W. Steubing, S. Cheng, W. H. Wright, Y. Numajiri, M. W. Berns, "Laser induced cell fusion in combination with optical tweezers: the laser cell fusion trap", *Cytometry* **12**, 505–510 (1991).

[140]. D. J. Stevenson, F. J. Gunn-Moore, P. Campbell, K. Dholakia, "Single cell optical transfection", *J. R. Soc. Interface* **7**, 863–871 (2009).

[141]. S. Kulin, R. Kishore, K. Helmerson, L. Locascio, "Optical manipulation and fusion of liposomes as microreactors", *Langmuir* **19**, 8206–8210 (2003).

[142]. A. Stromberg, A. Karlsson, F. Ryttsen, M. Davidson, D. T. Chiu, O. Orwar, "Microfluidic device for combinatorial fusion of liposomes and cells", *Anal. Chem.* **73**, 126–130 (2001).

[143]. J. M. Tam, C. E. Castro, R. J. W. Heath, M. L. Cardenas, R. J. Xavier, M. J. Lang, J. M. Vyas, "Control and manipulation of pathogens with an optical trap for live cell imaging of intercellular interactions,", *PLoS ONE* **5**, e15215 (2010).

[144]. D. J. Carnegie, D. J. Stevenson, F. Gunn-Moore, K. Dholakia, "Guided neuronal growth using optical line traps", *Opt. Express* **16**, 10507-10517 (2008).

[145]. M. Mathew, I. Amat-Roldán, R. Andrés, I. G. Cormark, D. Artigas, E. Soriano, P. Loza-Álvarez, "Influence of distant femtosecond laser pulses on growth cone fillopodia", *Cytotechnology* **58**, 103-111 (2008).

[146]. S. Suresh, J. Spatz, J. P. Mills, A. Micoulet, M. Dao, C. T. Lim, M. Beil, T. Sefferlein, "Connections between single-cell biomechanics and human disease states: gastrointestinal cancer and malaria", *Acta Mater.* **1**, 16–30 (2005).

[147]. M. Gu, S. Kuriakose, X. Gan, "A single beam near-field laser trap for optical stretching, folding and rotation of erythrocytes", *Opt. Express* **13**, 1369–1375 (2007).

[148]. J. Guck, S. Schinkinger, B. Lincoln, F. Wottawah, S. Ebert, M. Romeyke, D. Lenz, H. M. Erickson, R. Ananthakrishnan, D. Mitchell, J. Kas, S. Ulvick, C. Bilby, "Optical deformability as an inherent cell marker for testing malignant transformation and metastatic competence", *Biophys. J.* **88**, 3689–3698 (2005).

[149]. J. E. Curtis, J. P. Spatz, "Getting a grip: hyaluronanmediated cellular adhesion", *Proc. SPIE* **5514**, 455–466 (2004).

[150]. M. Andersson, A. Madgavkar, M. Stjerndahl, Y. Wu, W. Tan, R. Duran, S. Niehren, M. Mustafa, K. Arvidson, "Using optical tweezers for measuring the interaction forces between human bone cells and implant surfaces: system design and force calibration", *Rev. Sci. Instrum.* **78**, 074302 (2007).

[151]. W. Huang, B. Anvari, J. H. Torres, R. G. LeBaron, K. A. Athanasiou, "Temporal effects of cell adhesion on mechanical characteristics of the single chondrocyte", *J. Orthopaed. Res.* **21**, 88–95 (2003).

[152]. H. Liang, K. T. Vu, P. Krishnan, T. C. Trang, D. Shin, S. Kimel, M. W. Berns, "Wavelength dependence of cell cloning efficiency after optical trapping", *Biophys. J.* **70**, 1529-1533 (1996).

[153]. Y. Liu, G. J. Sonek, M. W. Berns, B. J. Tromberg, "Physiological monitoring of optically trapped cells: Assessing the effects of confinement by 1064-nm laser tweezers using microfluorometry", *Biophys. J.* **71**, 2158-2167 (1996).

[154]. S. Ayano, Y. Wakamoto, S. Yamashita, K. Yasuda, "Quantitative measurement of damage caused by 1064 nm wavelength optical trapping of Escherichia coli cells using on-chip single cell cultivation system", *Biochem. Biophys. Res. Commun.* **350**, 678-684 (2006).

[155]. K. C. Neuman, E. H. Chadd, G. F. Liou, K. Bergman, S. M. Block, "Characterization of photodamage to Escherichia coli in optical traps", *Biophys. J.* **77**, 2856-2863 (1999).

[156]. M. B. Rasmussen, L. B. Oddershede, H. Siegumfeldt, "Optical tweezers cause physiological damage to Escherichia Coli and Listeria Bacteria", *Appl. and Env. Microb.* **74**, 2441-2446 (2008).

[157]. G. Leitz, E. Fällman, S. Tuck, O. Axner, "Stress response in Caenorhabditis elegans caused by optical tweezers: Wavelength, power and time dependence", *Biophys. J.* **82**, 2224-2231 (2002).

[158]. N. K. Voulgarakis, A. Redondo, A. R. Bishop, K. Ø. Rasmussen, "Sequencing DNA by dynamic force spectroscopy: Limitations and prospects", *Nano Letters* **6**, 1483-1486 (2006).

1. Introduction

The continued interest of scientists in the study and understanding of the microscopic world has prompted new scientific and technological developments in optical **microscopy**, which has undergone a significant breakthrough in the last decades. Since the invention of microscopy in the 17^{th} century, a wide range of different imaging techniques have been developed and improved. However, a large period of almost 300 years, in which passive observation at the microscale was the only possibility, has elapsed since then. Several ingredients had to be available for the creation of the recipe that finally made possible the birth of the **optical tweezers** technique and the possibility to grab, hold and manipulate the samples under study: lasers, modular microscopes, fast silicon photodetectors, etc.

Thus, unsurprisingly, it was not until the 1970s, when Arthur Ashkin [1] discovered that **radiation pressure** (ability of light to exert pressure on material particles) could be harnessed to constraint the movement of small latex spheres, that the concept of optical trapping was invented and the manipulation of

microscopic samples using only laser light began to turn into a real possibility.

At present, several tools offer the combined advantages of manipulation and imaging, such as the scanning probe microscopes (AFM, STM), or close relatives of optical tweezers such as magnetic tweezers (MT) or dielectrophoretic (DEP) traps. However, optical trapping appears to be the most advantageous tool for the study and manipulation of microscopic samples (down to the nanoscale) in the force range between 0.1-100 pN. Distinctive features that make this technique stand out from others include non-contact force for cell manipulation, force resolution as accurate as 0.1 pN and amiability to liquid medium environments.

Biology, as a paradigmatic example, has found in optical trapping a goldmine of applications that have expanded its horizons and cross-fertilized with other sciences, such as physics, leading to improved understanding of single processes at the cellular and molecular levels. Biophysical research on single molecules that benefit from optical trapping technology include the study of molecular motors [2-5], protein conformational changes (folding / unfolding pathways) [6], protein-protein binding / unbinding processes [7], DNA-protein interactions [8] or DNA mechanical properties [9], to name a few. In addition, several applications have been developed for single cell experiments including cell transport, positioning, sorting, assembling and patterning [10]; cell nanosurgery [11]; optical guiding [12] and force measurements for the mechanical characterization of cells [13], or the study of intracellular processes in vivo [14]. In the physical sciences, optical tweezers have been widely acknowledged as a tool to study the physics of colloids, aerosols and mesoscopic systems [15-17], and in several applications in nanotechnology, such as manipulation and assembly of carbon nanotubes and nanoparticles [18,19].

Furthermore, for medicine and biomedical sciences, this new tool allows a jump back to basic and fundamental questions that had never been totally solved before, as well as an evident step forward towards the development of novel tools for diagnosis or treatment. Promising prospects that seem to be already in progress are found in the fields of in-vitro fertilization, cell-cell interaction, microbiology, immunology, stem-cell research, single-cell transfection, tissue engineering and regenerative medicine, among others.

The main purpose of this article is to paint the picture of optical trapping providing details or insights not commonly found in other –but still excellent– reviews [20-28]. The examples we resort to illustrate the work carried out at the Optical Trapping Lab - Grup de Biofotònica (BiOPT) of the University of Barcelona during the last years. This review does not pretend to be an exhaustive document but aims to give a view of the field from our particular standpoint. We will explain the basic mechanisms of optical micromanipulation with optical tweezers, followed by a description of our experimental setup based on holographic optical tweezers (HOTs) combined with epi-fluorescence microscopy. Then, we will explore the possibilities of the technique in performing quantitative measurements. Finally, we will discuss the biological advances brought about by this technology and conclude with the challenging, future prospects in the field. Other reviews [20-28] may offer a different perspective or contain complementary material and further references in various aspects of the field, so the interested reader is advised to also consider these as a reference.

2. Physical basis of optical trapping

Optical tweezers [29] use a highly focused laser beam to trap and manipulate microscopic (from nm to μm) neutral objects. In order to create the large spatial gradient in light intensity necessary to form a stable trap, a high-numerical-aperture (NA) microscope objective is required. The optical forces originated typically range between 0.1-100 pN.

Optical forces are light-matter interaction phenomena created by the momentum exchange between a light beam and an object with a refractive index ($n_{particle}$) different from that of its surrounding medium (n) ($n_{particle}>n$ for trapping). When the light beam passes through the sample undergoes a global momentum change which is

transferred to the sample (Newton's third law), resulting in a net force. Historically, this force has been split into two different components: the scattering force, which pushes objects along the direction of propagation of the light beam, and the gradient force, which pulls objects along the spatial gradient of light intensity. Three dimensional stable trapping can be achieved when gradient forces exceed those from scattering; thus, attracting the object to the point of highest intensity in the focused light beam. Despite the fact that the force decomposition into two terms is somewhat artificial for micron-sized particles, unlike the specific case of atoms, of much smaller size, for which the model was initially developed [30], the idea has remained in use due to the intuitive picture that it provides (see Box 1).

For a more rigorous description, one must resort to the Lorentz force equation. Albeit general, it has a simple formulation in terms of the Maxwell stress tensor ($\boldsymbol{T}$). In this case, the force per unit volume ($\boldsymbol{f}$) that the trap exerts on the sample is given by

$$\boldsymbol{f} = \frac{\partial \boldsymbol{p}_{mech}}{\partial t} = \nabla \cdot \boldsymbol{T} - \frac{\partial \boldsymbol{p}_{em}}{\partial t}. \qquad (1)$$

The light contributes in two different ways to the change in the momentum of the system: the divergence of the stress tensor and the change in the momentum of the electromagnetic wave ($\boldsymbol{p}_{em}$). In a trap, the first term is given by the intensity gradient of the scattered light $\nabla \boldsymbol{I}(\hat{\boldsymbol{s}})$ (see Eq. (2)), whereas the latter corresponds to the temporal variation of the Poynting vector $\boldsymbol{S}$ as $\boldsymbol{p}_{em}=\boldsymbol{S}/c^2$, where c is the speed of light.

In the opposite direction, the role that matter has in the variation of the light momentum remains unclear. The question of which is the exact expression for the momentum of the electromagnetic field in a material medium has been a subject of debate for a long time, which is known as the Abraham-Minkowski controversy [32]. A total consensus about this question does not exist yet as different experiments supporting two versions of the theory have regularly been reported. In practice, this has no effects in the experiments with optical traps since the observable quantity is not the variation in momentum of the electromagnetic field, but the net force ($\boldsymbol{f}$) felt by the particle.

BOX 1. INTUITIVE DESCRIPTION

When the trapped particle is much larger than the light wavelength (ray optics regime), a simple explanation for the optical forces emerges by looking at the beam deflection. The deflection of each ray when passing through the object creates a force acting on the particle, due to the momentum conservation law.

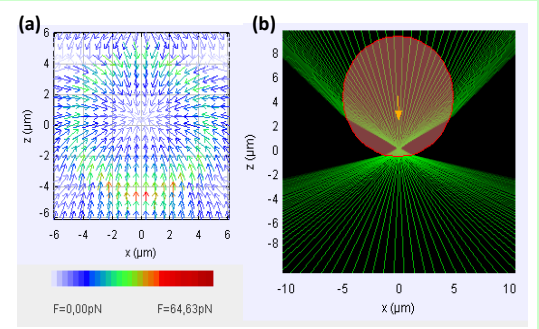

If a high-numerical-aperture focusing lens is used, a stable trapping position is created close to the focus of the beam. Figure (a) illustrates a 2D simulation of the optical force field experienced by a polystyrene spherical particle (refractive index = 1.58, diameter = 10 μm) suspended in water (refractive index = 1.33). The beam in the simulation has a high numerical aperture (NA = 1.3) and propagates towards the positive z direction. Figure (b) shows intuitively how radiation pressure on such a beam can create a restoring force in the axial (z) direction, instead of just pushing forward the particle. Notice that when the particle is positioned slightly above the focus (0,0) of the beam, the refracted light cone closes, and the beam gains axial momentum (in the positive z direction). Hence, the particle feels a negative axial force (towards the focus) due to momentum conservation. Incidentally, a similar behaviour is observed when the particle is positioned out of the focus in the transverse (x) direction. Due to the same principle, the beam deflection creates an x-restoring force which also points towards the trap centre.

Simulations were performed with a Java application [31] developed by us. The complete source code and the executable file can be downloaded from:

http://code.google.com/p/optical-tweezers/.

If we now extent Eq. (1) to a sample with volume V, the optical force is obtained as the sum of f over the whole volume:

$$\langle \boldsymbol{F} \rangle = \int_V \langle \boldsymbol{f} \rangle dv = \int_V \langle \nabla \cdot \boldsymbol{T} - \frac{\partial \boldsymbol{p}_{em}}{\partial t} \rangle \, dv =$$

$$= \int_S \frac{n}{c} \boldsymbol{I}(\hat{\boldsymbol{s}}) \cdot \hat{\boldsymbol{s}} da. \qquad (2)$$

ETHER

The expression for the force given in equation 1 is formally equivalent to the Navier-Stokes equation for a fluid of negligible density. This makes sense, since according to Maxwell's hypothesis (supported by many other eminent scientists), 'ether' was the undetectable fluid that worked as a means of support for electromagnetic radiation. As it is known, its existence was generally rejected after the Michelson-Morley experiment and, although Maxwell's theory was entirely based on this assumption, surprisingly neither modifications of the original formulation have been necessary nor evidences of the presence of ether have been found.

where the angular brackets denote a time average and the integral over S is carried out on a closed surface enclosing the particle, with defining the outward unit vector normal to the integration surface. The second term in the integral disappears because the time average of the Poynting vector vanishes for intensities that are constant in time [33]. The optical force expressed in these terms is entirely determined by the electric and magnetic fields at the surface S, for the specific case of a rigid object, where n is the index of refraction of the propagation medium. Intuitively, the net force can be considered pointing towards the centre of mass of the scattered light distribution over this spherical surface.

The theoretical calculus of the optical force from the former expression is far from trivial, since the computation relies on the angular distribution of the scattered intensity, which is, in general, quite complex (Fig. 1). When solved, however, the formula provides accurate and rigorous results. The solution to general problems with no particular symmetries or with arbitrary laser illuminations requires the use of the T-matrix formulation, which is computationally tedious [34]. Special cases of plane-wave scattering by spherical particles, or its more general version with arbitrary fields, can be addressed with the simpler Lorenz-Mie and Generalized Lorenz-Mie theories [35], respectively. Even so, the resolution of these problems is still complicated. Different computational codes to calculate the optical forces in these cases are available and can be freely downloaded from the internet: (e.g., http://www.physics.uq.edu.au/people/nieminen/software.html [34]).

Fortunately, there are two cases for which useful information can be extracted from a simplified analytical theory. These correspond to the limits of tiny and large spherical particles (see Box 2). The mathematical treatment describing the light-particle interaction is different depending on the ratio between the dimension of the trapped particle (radius r) and the wavelength (λ) of the trapping laser source. First, if we consider a dielectric particle whose radius is much smaller than the wavelength, the particle may be considered as an oscillating dipole and the appropriate mathematical formulation to be used is the Rayleigh limit [36], which describes particle-light interactions using wave optics. On the other hand, for cases where the particle size significantly exceeds the trapping laser wavelength, the Mie limit or geometric / ray optics regime [37] suffices to describe the phenomena of optical forces, which

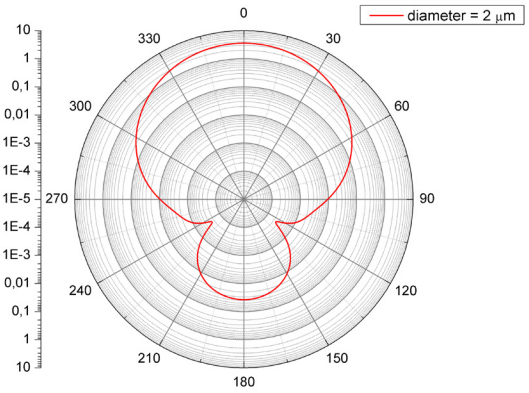

Fig. 1. T-matrix scattered intensity polar diagram in arbitrary units of a 2 μm bead illuminated by a Gaussian beam (beam waist ω_0 = 0.4 μm).

can be shown to result from refraction and reflection.

An important result is that, independently of the particle size, it can be proved that the tightly focused laser beam creates a parabolic potential energy well for the trapped object in the vicinity of the focus. This potential landscape implies that for small displacements away from the trap centre, the force is directly proportional to the displacement (x), thus creating a simple but powerful way of converting any displacements observed into measurements of force (F) (Fig.

BOX 2. LIMIT REGIMES

Rayleigh regime ($r<<\lambda$)

This regime provides an analytic solution to the problem of optical trapping and is the case that accepts a deeper analytical treatment. Although the dipole approximation is far from acceptable in most of the experiments, the results from this theory provide at least a flavour of the behaviour of optical traps. Additionally, the Gaussian modelization of the trapping beam is often introduced for a further development of the formulation, which leads to explicit equations for the force in terms of the different experimental parameters [36]. However, it should be kept in mind that although frequently used [36,38], the applicability of these results is limited. For Gaussian beams, these approximations are dependent upon the following requirements:

1) The dipole model demands a homogeneous electric field over the whole sample, which leads to a constraint on the size of the particle $r<\omega_0$ (where ω_0 is the beam waist) in the expression for the lateral component of the force. However, as Harada et al. have shown [36], the largest discrepancy appears in the axial force, which is only truly well described by Rayleigh expressions for $r<\lambda/20\sim50$ nm.

2) On the other hand, the model only applies to low-convergence beams, leading to an error less than 5% for $NA=n_m\sin\theta_{max}\leq0.5$ ($\theta_{max}\leq30^o$), where NA is the numerical aperture of the objective used to focus the beam, n_m is the refractive index of the immersion medium and θ_{max} is the maximum angle of the rays generating the trap. This corresponds to a beam waist of at least $\omega_0=\lambda_0/\pi NA=0.68$ μm, larger than $\omega_0=0.4$ μm, typically used in experiments [20,39].

Mie regime ($r\geq5\lambda$)

The main interest of the ray-optics regime lies in the simple and intuitive image that it provides on how optical tweezers work, as previously shown in the beginning of the present section (see Box 1). It is also feasible to obtain an analytical expression for the force as a function of different experimental parameters [37], but unfortunately only encompassing a single ray. Any further result (for example, force exerted by the whole trapping beam) requires reiterating the computation.

2a). The trap is akin to a small spring obeying Hooke's law: $F=-kx$, where k is called trap stiffness. As we will show below (see section 4), this indeed confers optical tweezers the possibility, not only of manipulating microscopic samples, but also of measuring the small forces involved at this length scale. There exist several

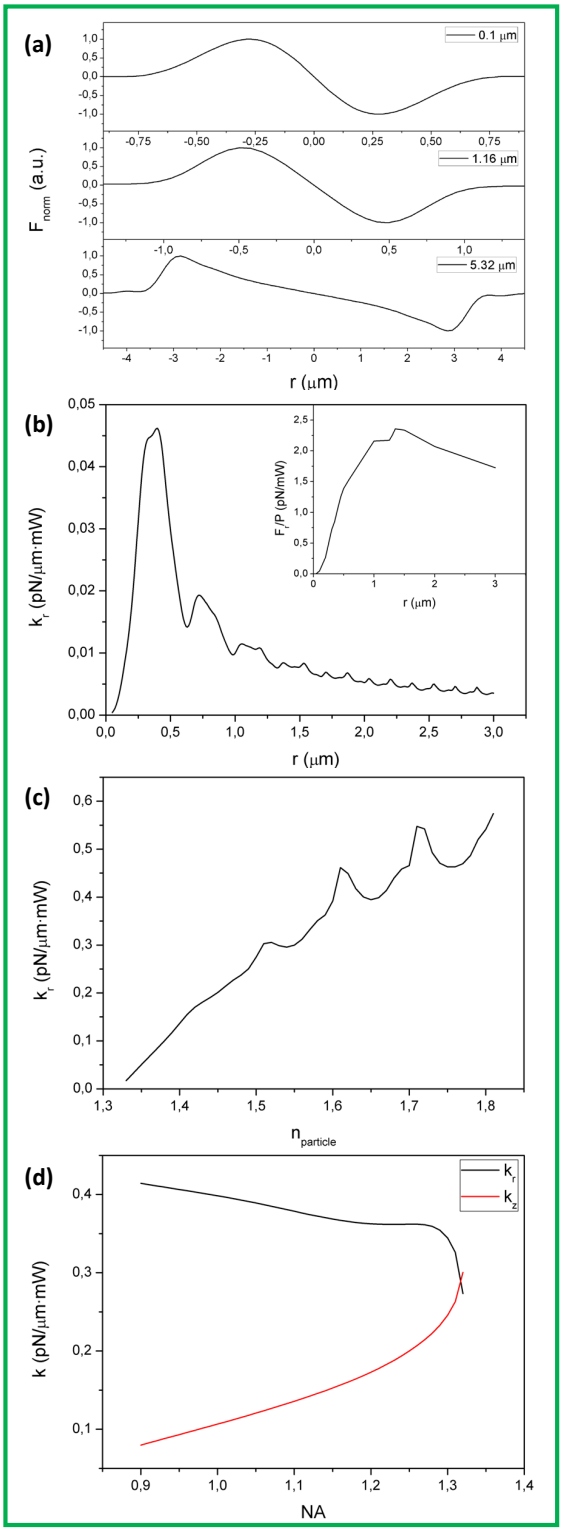

Fig. 2. Simulation of the trap stiffness (radial k_r and axial k_z) as a function of different parameters: (a) the distance from the centre of the trap for different particle sizes, (b) the particle size, (c) the particle's refractive index, and (d) the microscope objective numerical aperture.

experimental parameters that affect the value of *k*, such as the particle's radius, the ratio between the refractive indices of the particle and the surrounding medium, the numerical aperture of the microscope objective or the laser power (Fig. 2). Consequently, a calibration in situ for the trap stiffness must be performed for every single experiment.

3. Holographic optical tweezers

Different configurations exist for generating an optical trap. Two counter-propagating laser beams can create a stable trap by compensating their pushing axial forces while creating a strong transverse force. However, the single beam configuration, which employs a single high-numerical-aperture laser beam to obtain a stable trap, is the most common, since it can be easily adapted to a conventional epi-fluorescence microscope (see Box 3), while conserving its advanced imaging capabilities. This way, optical tweezers can be used for micromanipulation experiments while performing high quality imaging of the sample, which is usually necessary when dealing with biological specimens.

A further step in the manipulation of the microscopic world is to control a plurality of optical traps at the same time. This possibility allows the simultaneous trapping of several microscopic samples, as well as to take hold of a larger object from different points in order to control its position and orientation during an experiment [40]. The use of several optical traps would be an equivalent to our fingers in the microscopic world, by adapting their position to the three-dimensional shape of the grabbed object. There is a growing need and interest in the use of more than one trap for manipulation, in important fields such as single molecule biophysics [23]. The "dumbbell" configuration, which is increasingly being used in several assays for characterizing motor proteins [41], requires two independent traps. A more sophisticated example is found in [42], where the preparation of the experiment requires that four traps are used to hold two DNA strands and wound one of them around the other.

There are different methods to generate multiple optical traps, either by combining independent laser sources into the objective lens, splitting a single laser beam into two orthogonally-polarized beams or creating interferometric patterns of light spots from a single beam. Unfortunately, these solutions are either expensive, restricted to two traps or to fixed trap patterns, respectively.

In contrast, the most useful approaches for generic micromanipulation experiments are those offering a dynamic and versatile control over an arbitrary number of independent traps. For that purpose, one can use a **time-sharing technique**, which consists of a fast switching of the laser beam between different positions in the sample (as much as the number of desired optical traps). If the switching is performed quickly enough, the trapped objects do not see the flickering and apparently behave as in a constant laser spot.

Time-sharing can be implemented with different devices, such as acoustooptic deflectors, scanning galvanometer mirrors or electrooptic deflectors. Their performance in terms of speed, position repeatability, range of deflection angles, beam pointing stability or optical efficiency is uneven, each of them being strong in certain aspects and weak in others [44]. High-speed beam deflection for time-shared optical traps is usually computer-controlled, and the intensity and 2D-position of each optical trap can be tuned independently. However, the number of traps cannot be increased indefinitely, since the visitation frequency for each trap should be high enough to prevent particles from escaping. Although 1000 visitations per second per trap are adequate in most cases, in [45] it is shown that a visitation rate of 10 kHz per trap would be necessary for bringing the diffusion distance between laser visitations down to 1 nm, thus limiting the number of traps to only six in that case. Such accuracy is convenient in precise experiments as, for example, in molecular motor studies.

A recent, innovative approach to generate multiple traps is the use of digital holography for spatially modulating the laser beam, adding in-depth control of the multiple traps, in contrast to

the 2D positioning performed by deflecting-only devices. Holography was first introduced in the field of optical micromanipulation in 1998 [46], by adding a liquid crystal spatial light modulator (SLM) in the optical path of the trapping laser. The SLM is a reconfigurable device allowing the modulation of the phase and/or amplitude of an incident light wavefront at each pixel of the display. In this way, one can control, for example, the tilt and convergence of the output wave, or split the beam into many beams at different angles. Consequently, custom positioning of an arbitrary number of light spots in the sample plane (after the focusing, objective lens) is achieved, and thus micro- and nanoparticles can be trapped and manipulated in 3D, with no need for mechanical movements in the optical elements of the setup. So far, holographic optical tweezers have found abundant applications in microfluidics, biophysics, colloidal studies, and 3D micromanipulation experiments in general [26].

A typical SLM basically consists of a cell filled with an optically anisotropic material (such as a nematic or ferroelectric liquid crystal, see Fig. 3) in which each pixel responds to an external applied voltage by changing its optical properties, introducing a spatially controlled phase and / or amplitude modulation in the light wavefront. Digital holograms are matrices of gray-level values that are converted to voltage signals by the SLM controller, via the graphic board of a driving computer. The gray level to phase / amplitude response curve of the SLM

BOX 3. EXPERIMENTAL SETUP

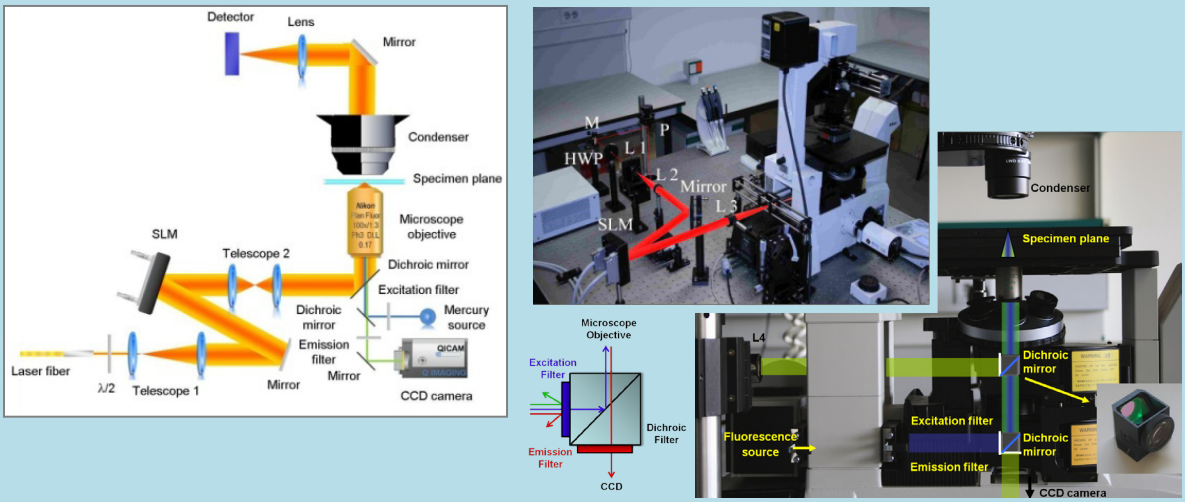

Our optical tweezers system consists of a continuous-wave (CW) Ytterbium fiber laser with a Gaussian beam profile (TEM00) that emits up to 5 W at a wavelength of 1064 nm. A half-wave plate rotates the linear polarization of the beam for proper operation of a spatial light modulator (SLM, Hamamatsu X10468-03), which is responsible for the generation of the holographic traps. Two sets of telescopes are used for pupil matching: telescope 1 adjusts the beam size to the active area of the modulator (or slightly overfills it), while telescope 2 images the SLM on the entrance pupil of the objective. Finally, the laser beam enters the microscope (Nikon Eclipse TE2000-E) through a rear port, reaching an objective lens of high numerical aperture (Nikon CFI Plan Fluor 100x oil immersion, 1.3 NA, or Nikon Plan Apo VC 60x water immersion, 1.2 NA), which tightly focuses the laser beam at the specimen plane and also images the sample on a CCD camera (QImaging, QICAM). A dichroic mirror placed before the objective lens reflects the laser light up while transmitting down the illumination light coming from the condenser to the camera. By means of a graphical user interface, traps can be dynamically created, moved and deleted to perform the experiments conveniently [43].

The microscope is equipped with two filter turrets to allow simultaneous generation of optical traps and epi-fluorescence microscopy. A mercury source (Nikon Intensilight C-HGFI) is used in conjunction with a filter cube (or optical block), including an excitation filter, a dichroic mirror and a barrier (or emission) filter. Note that the upper dichroic mirror needs to be transparent to the excitation light towards the sample and to the emitted light from the sample. At the same time, if we want to observe the trap, a certain amount of infrared laser light from a back reflection needs to reach the camera after going through the two dichroic mirrors and the emission filter. Often, the trap is so intense that an extra filter blocking infrared light is added before the CCD to avoid saturating the sensor.

needs to be determined or a priori known when computing digital holograms. The SLM is usually positioned in a conjugate plane of the back focal plane of the focusing lens (see Box 3), so that the modulated wavefront and the final light distribution in the front focal plane of the lens are related by a Fourier transform. Thanks to this relation, the custom modulation of the beam phase and amplitude profile that produce the desired arbitrary 3D trap patterns in the sample plane can be computed. In Fig. 4, two simple cases of phase modulation are illustrated.

To create complex and arbitrary optical traps distributions, several algorithms exist that compute the digital holograms to be encoded on the SLM. The choice of the appropriate algorithm depends on the requirements of the experiment in terms of optical efficiency, precision in the trap position or intensity, or computational speed. For instance, two of the standard methods are the Gerchberg-Saxton algorithm [47] and the prisms-and-lenses algorithm [48], which are based on the ideas shown in Fig. 4. Whereas the former has a high efficiency but also a high computational cost and is therefore rarely used in in-line computations, the latter involves a lower computational load and is easily implemented in real time, in dynamic micromanipulation experiments. However, it produces holograms with lower optical efficiency.

Figure 5 shows several possibilities of holographic optical tweezers: it allows dynamically splitting a laser beam into a plurality of optical traps (Fig. 5(a)), manipulating them independently (Fig. 5(b)), as well as **controlling the depth of each light spot** (Fig. 5(c)). Another advantage brought about by holography is the possibility to **correct for optical aberrations** to improve trapping performance [49-52]. Furthermore, twin traps with different focusing depths can be generated [53] allowing single beam optical tweezers to trap even at low numerical apertures. Another interesting application is the creation of **optical traps with exotic shapes and properties**, like Laguerre-Gaussian beams, which carry light orbital angular momentum that makes the trapped particles rotate within a light vortex, as shown in Fig. 5(d).

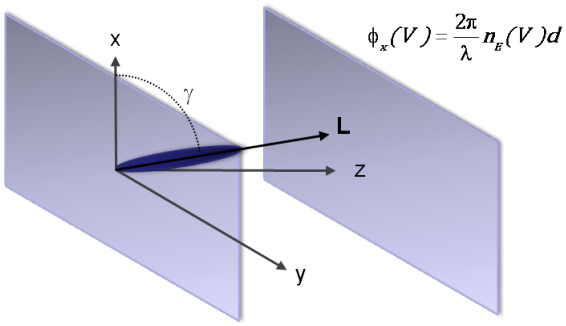

Fig. 3. In commonly-used SLMs, a cell is filled with nematic liquid crystal molecules and a voltage V is applied at each pixel (x,y) through transparent electrodes situated at the enclosing surfaces. Liquid crystal molecules optically behave as a uniaxial material having an optical axis L, which tilts an angle $\gamma(V)$ as the molecules tend to orientate with the applied electric field.

An incoming linearly polarized light in the x direction propagates in the cell with an apparent refractive index n_E that depends on the angle $\gamma(V)$ between the direction of propagation (z) and the optical axis L. Thus, the incoming wave suffers a phase delay $\phi_x(V)$, which can be tuned by changing the applied voltage. This tilt effect leads to phase-only modulation (suitable for generating most of the desired light distributions), since light amplitude of the incoming wavefront is unaltered while passing through the liquid crystal cell (though there is always a little, inevitable absorption). The SLM response is polarization dependent as, for example, a linearly polarized beam in the y direction would always experience the same index of refraction n_O, independently of the orientation of the molecules.

The scheme shown here corresponds to a parallel nematic liquid crystal SLM. However, in twisted nematic liquid crystal SLMs a rotation (twist) of the molecules from the input to the output surface is induced and other effects need to be considered. A coupled modulation of the amplitude and phase is generally induced, and the complex response of the SLM must be taken into account during hologram preparation, in order to optimize holographic modulation efficiency.

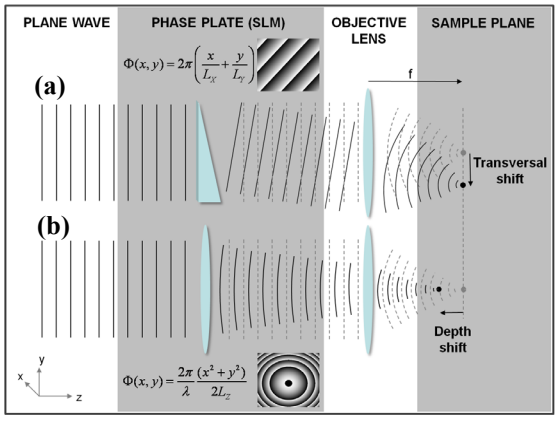

Fig. 4. (a) A linear phase deviates the incoming plane wave, as a prism would do, causing a transverse shift to the trap in the focal plane of the objective lens (in the example, the y direction is shown, the shift being inversely proportional to the period of the linear phase, L_y). (b) A spherical phase acts as a lens and converts the incoming collimated beam into a convergent or divergent beam, such that the trap is focused before or after the sample plane, respectively.

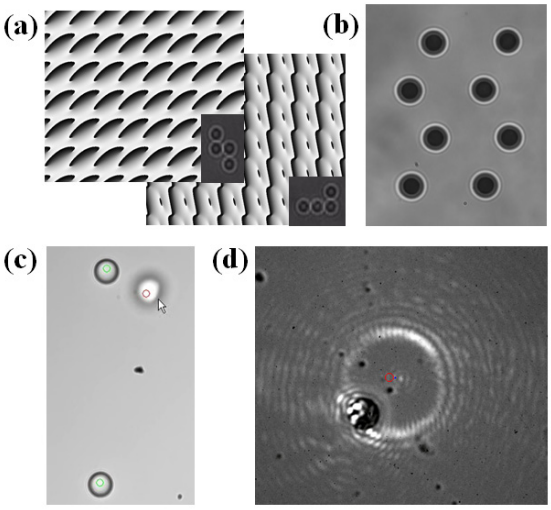

Fig. 5. Examples of holographic manipulation with optical tweezers. (a) Computer generated holograms obtained with the Gerchberg-Saxton algorithm encoding two different 4-trap configurations. The insets show the resulting pattern, in which 1 μm polystyrene beads dispersed in water are trapped at the same time. (b) Frame extracted from a video sequence in which eight optically-trapped 3 μm polystyrene microspheres are moved independently. (c) Frame extracted from a video sequence in which 3 polystyrene microspheres are holographically trapped. One of the beads is holographically moved to a different focus while the other beads remain stably trapped at the original plane. (d) Snapshot of a video sequence showing a particle trapped in a vortex ring. The angular momentum makes the particle rotate, while the upper coverslip of the containing microchamber confines the movement in depth

Advances of the technique in the last decade have led to the implementation of devices with convenient interfaces, which make micromanipulation as simple as sliding the operator's hands over a multitouch screen [54], allowing us to reach and operate in the microscopic world as easily as in the macroscopic world.

The main limitation of holographic optical tweezers, which restrains at present its potential, is the difficulty of using them as force sensors, due to a certain lack of stability [55,56] and the complexity of simultaneously calibrating the stiffness of several optical traps. This usually requires the use of sophisticated high-speed cameras instead of the inexpensive position sensing detectors commonly used in single-beam optical tweezers, as we will see in the following section. Nevertheless, some effort has been put through in the last years to widen the functionalities of holographic optical tweezers from dynamic micromanipulation to precise quantitative measurements [49, 55].

4. Force measurements

Despite the impressive manipulation capabilities of matter at the microscale provided by optical trapping technology, its impact on many fields of scientific importance would have been much less had it lacked a quantitative side. Indeed, the effect caused by an optical trap can be measured with great accuracy and this allows exerting controlled forces onto the captured samples and performing experiments with minute detail and resolution.

Usually, force measurements (F) with optical tweezers are indirectly obtained from the measurement of the position of the sample in the trap (x), as outlined in section 2. Within a region of some hundreds of nanometers around the equilibrium position ($x<<\omega_0$), the potential energy of the sample follows a parabolic equation and the trap behaves harmonically, as a putative "optical" spring. Thus, the restoring force that keeps the particle in a stable position is linear with displacement (x) so that it can be described by an optical equivalent to Hooke's law. Hence, force measurements are usually split into two separated steps: the **determination of stiffness** k, or trap calibration, and the measurement of the relative displacement of the trapped particle x. The product of the two magnitudes provides the force. As a result, the development and improvement of different calibration methods for the trap stiffness and the adaptation of position detection techniques to measure sample displacements have been of paramount importance. We discuss the state of the art in this field along these two lines.

On the one hand, methods inspired in differential interference contrast (**DIC**) imaging [57,58], **video-based position detection** [49,62] or back-focal-plane (**BFP**) interferometry [44,38,63-65] are prominent examples of methods to properly determine the sample displacements. Back-focal-plane interferometry is a distinctive approach, specifically developed for this task, through a somewhat intertwined evolution from other methods (see our attempt at a timeline in Box 4).

BOX 4. POSITION MEASUREMENT IN OPTICAL TRAPS: A DEVELOPMENT TIMELINE

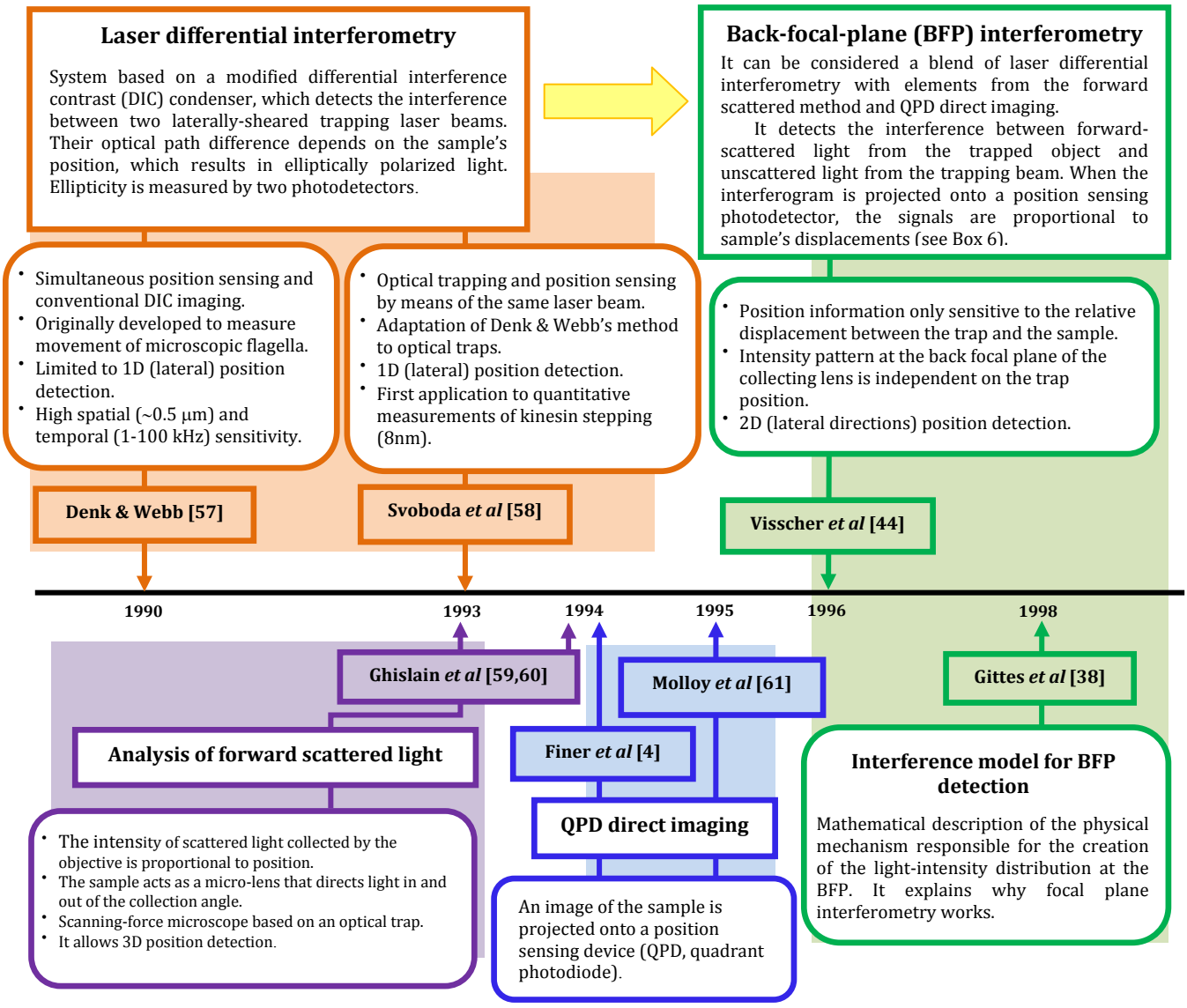

It is currently the most popular position detection scheme due to its straightforward implementation and high spatial (< 1nm) and temporal (kHz) resolution. The system analyzes the light that comes from the trap after it has crossed the sample, extracting its positional information. We summarize its main features in Box 6.

On the other hand, several methods can be used for the determination of the trap stiffness that is for the calibration of the optical trap, all of these presenting strengths and drawbacks. They are all conceptually similar in that they essentially consist on the application of known forces and the determination of their effect on the trapped particle. It is clear that stiffness can be determined when both the forces and the elicited displacements are simultaneously known. The actual procedure, however, might be complex since the force is sometimes only known in a statistical sense. Basically, we can divide the methods in two different types, hydrodynamic or thermal, depending on the origin of the external force used to calibrate the trap [67]. The **drag force method** [68-70] analyses changes on the position of the trapped

BOX 5. TRAP STIFFNESS CALIBRATION: POWER SPECTRUM ANALYSIS

The analysis of the **power spectrum** of the Brownian motion of a trapped particle provides accurate information about the trap parameters. Indeed, the expected one-sided power spectrum (only accounts for positive frequencies of the symmetric power spectrum) has the following expression,

$$P(f) = \frac{2\left|\hat{x}(f)\right|^2}{T_{msr}} = \frac{D/\pi^2}{f^2 + f_c^2} \quad , \qquad (1)$$

Experimental determination of corner frequency f_c provides the stiffness

where T_{msr} is the recording time, $D = K_B T/\gamma$ is the diffusion coefficient, $\gamma = 3\pi\eta d$ is the Stokes' drag of the particle with diameter d in a solvent with viscosity η, K_B is the Boltzmann constant, T is the absolute temperature, $f_c = k/2\pi\gamma$ is the corner or roll-off frequency of the spectrum, and k is the trap stiffness.

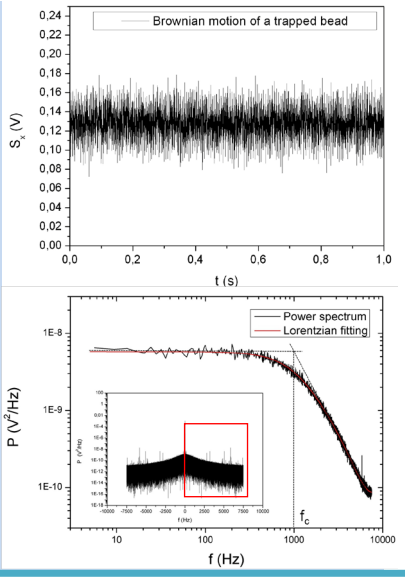

The photodetector records the relative displacement $x(t)$ of the trapped particle for a time T_{msr} as an electric signal $S(t)$, in volts, for example by means of back-focal-plane interferometry. This time-domain data has Gaussian probability distribution, typical of the Brownian motion of a particle in a harmonic potential. However, a frequency-domain description provides substantial advantages for interpreting continuous phenomena, such as oscillations and stochastic noise signals. Therefore, thermal noise is best characterized by its power spectrum $P(f)$, in V^2/Hz units, which is obtained by taking the squared magnitude of the Fourier transform from the original time-domain data. In our case, $P(f)$ has the characteristic shape of a Lorentzian function (eq. 1 above). From the corresponding fitting, we obtain a value for the corner frequency f_c and, assuming that the Sokes' drag on the particle is known, **the trap stiffness k can be calculated**.

The corner frequency f_c divides the Brownian motion into two distinct regimes. For $f << f_c$, the power spectrum exhibits a constant region (plateau of value $D/\pi^2 f_c^2$), which reflects the confinement of the particle. At $f >> f_c$, $P(f)$ falls off as $D/\pi^2 f^2$, which is characteristic of free diffusion (at short observation times, the sample moves as the trap did not exist).

Data logging and fitting corrections

Accurate trap calibration requires a very precise modelling of the power spectra. Some of the effects that may cause a measurable error [66], and which should be corrected, are:

- **Aliasing**: effect generated by sampling of the power spectrum with finite sampling rate (f_s), which limits the highest frequency component to be unambiguously measured to $f_{Nyq}=f_s/2$. As a result, power spectral density at frequencies above f_{Nyq} is folded back to lower frequencies below the Nyquist frequency.

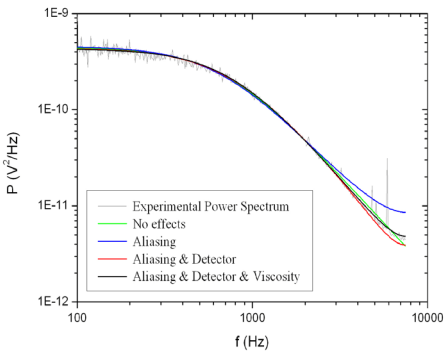

- **Position detection system is a low-pass filter**: signal filtering during data acquisition due to electronic filters or parasitic filtering by the photodetector leads directly to a numerical underestimate of the roll-off frequency and thereby to the stiffness of the optical trap. Errors introduced by low pass filtering become severe as the roll-off frequency of the trap approaches the roll-off frequency of the electrical filter.
- **Frictional force dependent on trapping depth**: the friction coefficient depends on the hydrodynamical interaction between the sample and the coverslips that close the chamber. Thus, the distance between these must be large or the effect should be corrected through Faxén formula.
- **Cross-talk between channels**: an asymmetric light scattering or difference in sensitivity in the elements of the photodetector may cause the 'x' and 'y' channels to couple, thus, it is important to decorrelate them.

particle as a function of a known viscous force, applied by moving the sample at a controlled speed through the suspension liquid (often justwater), by means of a motorized stage. Despite being the most direct method for the determination of the trap stiffness, drag-force measurements are less reliable than those based on the thermal motion of the particle and require expensive piezoelectric stages. The alternative is the analysis of the Brownian

BOX 6. POSITION DETECTION: BACK-FOCAL-PLANE INTERFEROMETRY

The **BFP interferometry** technique analyses the light coming from the optical trap after passing through the sample with a position sensing photodetector, typically a quadrant photodiode (QPD). If the QPD is placed at the back focal plane of the collection lens, the signal can be shown to be proportional to the relative displacement of the trapped particle.

1 Experimental setup

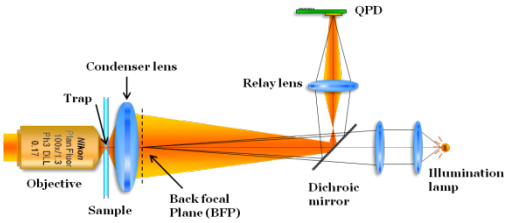

The light is collected with a lens (condenser) that is also used to illuminate the sample. A dichroic mirror, placed after this condenser, reflects the light coming from the trap and allows the illumination light to go through and reach the sample. The system is designed to project the light pattern at the BFP of the collection lens onto the detector by an auxiliary lens (relay lens).

2 Light pattern at the BFP of the collection lens

When the size of the particle is smaller than the wavelength of the laser, the sample behaves as a dipole (Rayleigh). Hence, the light passing through the trapped particle is scattered, creating a new spherical wave. Then, the light leaving the trap has two different contributions: the light scattered by the sample and the unscattered light from the trapping beam. Both terms are collected by the condenser and interfere at its BFP, forming interferograms similar to that in the figure below.

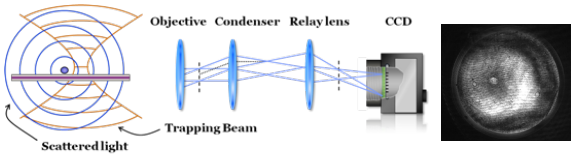

Essentially, the field at the BFP of the lens is the Fourier transform of the field at the sample plane. This configuration has some advantages when detecting the position of a sample.

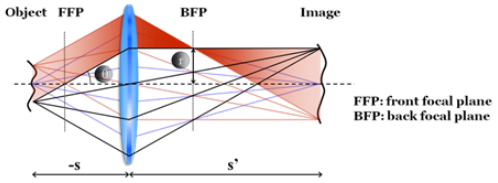

Specifically, any change in the position of the object generates an undetectable shift in the phase of the field at the BFP of the lens. The BFP of the condenser does not provide any information on the absolute position of the trap within the sample, but it does contain information about the **relative distance between the trapped particle and the laser beam, which is exactly the required information to compute the force**.

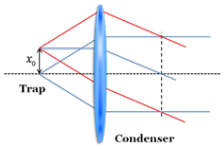

3 Photodetector: QPD

A quadrant photodiode is a silicon detector whose surface is divided into four quadrants that behave as independent detectors, providing voltages V_i that depend on the intensity of the illuminating light. The QPD produces three overall signals S_x, S_y and S_z which are linear combinations of the four individual detector voltages V_i (image below). S_x and S_y depend linearly on the position of the light spot on the surface of the detector. Therefore, these two signals provide a measure of the position *(x,y)* of the beam. Additionally, S_z is a signal proportional to the total intensity of the beam.

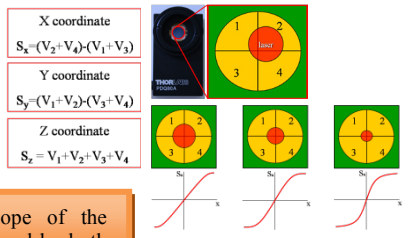

The **QPD sensitivity** (slope of the linear region) can be increased by both reducing the size of the spot or increasing the NA of the condenser.

4 QPD calibration: Signal-position curve

As shown by Gittes and Schmidt [38], when the interferograms at the back focal plane are integrated by a QPD, the signals are proportional to the particle displacements within certain limits. The figure below shows the signal from a position detector in a BFP configuration when scanning a latex microbead through the laser beam along the transverse direction *r*, by a piezo stage. The recorded signal S_x is proportional to the position of the particle, for small displacements ($x << \omega_0$):

$$x = \beta S_x \qquad (1)$$

Thus, two constants, β and k, must be experimentally measured to calculate the force from the detector signal S_x according to:

$$F = -k\beta S_x \qquad (2)$$

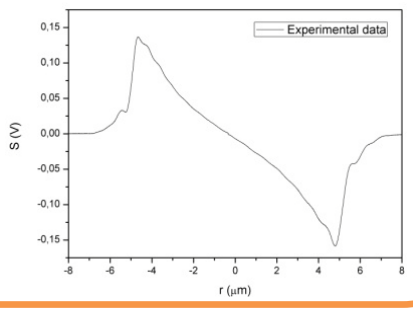

motion of a trapped object, where no external force source is necessary. Two methods may eventually deliver the stiffness: the **equipartition theorem** [71], which provides a fast estimation, and the **power spectrum analysis** [66], which seems to be the most accurate and reliable one. We give the details in Box 5.

Berg-Sorensen and Flyvbjerg have studied with detail the acquisition and accurate fitting of the Lorentzian to derive the trap stiffness [66], developing a realistic expression for the experimental power spectra, which includes several corrections (see Box 5). Calibration accuracy down to 1-2% error requires accounting for an exhaustive list of different phenomena, which range from variations in the hydrodynamic friction of the trapped particle, due to the proximity of the coverslip, to parasitic filtering in the photodiode due to transparency of silicon at the infrared wavelengths of the trapping lasers. Fortunately, they have developed and made a freely available MATLAB program that allows a comfortable plotting and fitting of the experimental data [72]. Besides determination of the trap stiffness, acquisition and observation of the power spectrum is also useful as a diagnostic and debugging tool for optical trapping equipment: it allows detection of alignment errors from either the optical trapping or the position detection system, and detection of external sources of instrumental noise. Additionally, it can also be used to monitor heating of the sample due to partial absorption of the trapping laser light [73].

Although extremely successful and widely applied, force determination based on these two pillars, calibration of the trap through the power spectrum method and position measurements by back-focal-plane interferometry, is only valid within narrow experimental conditions. The approach requires the use of non-aberrated Gaussian beams, spherical particles and optically and mechanically homogeneous viscous media. As a result, a significant amount of important experiments, ranging from the manipulation of irregular samples to in vivo cellular studies (such as intracellular vesicle trafficking by molecular motors), are currently out of reach from optical trapping technology.

The search for solutions to the problem as well as for an alternative method for direct force determination has increasingly become an important challenge. Some progress has been made in the calibration of non-harmonic potentials [71,74] or inside buffers with arbitrary viscosities [75], and also in BFP interferometry, by allowing the use of non-spherical particles or the presence of additional structures blocking the beam [76,77]. On a parallel track, Smith *et al.* [78] developed an improved version of their technique for direct force detection, proposed as early as 1996 [9]. It is based on the analysis of the momentum change of the trapping beam, which is directly related to the optical force generated by the trap through Newton's laws. This method does not depend on the experimental conditions since it is based on first principles, so that changes in the particle's geometry, the beam's intensity profile, and the viscosity and refractive index of the medium do not alter the measurements. It is important, however, to collect all the scattered light in order to correctly assess the amount of momentum change and, thus, the earlier experimental setups demanded the use of low-numerical-aperture trapping beams, arranged in a counter-propagating geometry. This constraint made compatible with single-beam optical traps, which are more flexible and used than counter-propagating traps, thus opening new avenues for advanced experimentation.

5. Biological applications

From Ashkin's first attempt in 1987 to manipulate biological samples, particularly viruses and bacteria, with infrared optical tweezers [80] and as he predicted when interviewed in 1997 at AT&T Bell Laboratories [81], researchers have developed a broad spectrum of different methods that use optical tweezers to perform both qualitative studies and quantitative measurements on biological specimens. This is possible because the forces typically exerted by optical tweezers, which vary between 0.1-100 pN, as well as the characteristic length scales, ranging from nanometres to hundreds of micrometres, and time scales down to the microsecond, cover a similar range as those responsible for many processes in biology

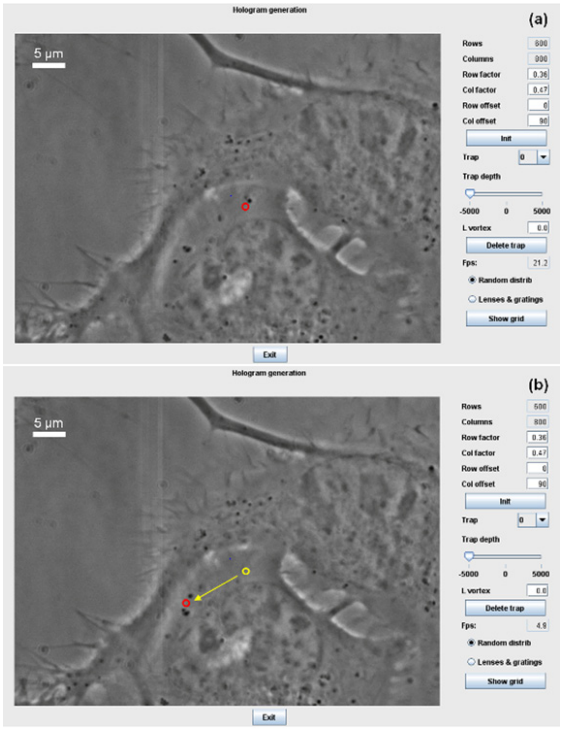

Fig. 6. **Holographic manipulation of sub-cellular structures in living NG-108 cells**. The sequence of images (extracted from a video) shows the real-time manipulation of a ~ 750 nm free body across the cytosol of the cell, by means of our holographic optical tweezers system. As seen in the image, optical traps can penetrate the cell membrane, reaching the cytosolic structures without puncturing or otherwise damaging the cell. The arrow represents the total displacement of the vesicle and the red circle indicates the position of the laser trap. The experiment was carried out by using our application, HoloTrap [43], an interactive tool for creating, moving and removing optical traps quickly just by clicking and dragging the mouse.

Intracellular transport in eukaryotic cells requires the proper action of three sets of transporters: myosin, kinesin and dynein motors. Molecular motors are dimeric proteins that can "walk" along the cytoskeleton of the cell by detaching and reattaching their motor domains (heads), successively with a fixed step size.

Using the energy derived from the ATP hydrolysis as a "fuel" source, these enzymatic motors pull the displaced cargos throughout the cell processively, in a persistent way, exerting forces of a few piconewtons.

Recently, we have adopted a high-speed tracking methodology to detect motor stepping events in living cells by means of a back illuminated, electron-multiplying (EM-CCD) camera. This device, which is designed for a high sensitivity at low exposure times, is used to monitor the centre of mass of motor-driven cargos, with nanometre accuracy, and, ultimately to study the action of molecular motors, which still remains poorly studied in vivo. The optical manipulation of motor-driven vesicles allows a mechanical interaction with their associated transport proteins [82]. The capability to resolve nanometric steps combined with a force measurement technique that we have developed [79] could pave the way to characterize the mechanics of motor proteins inside living cells.

(inter- and intracellular processes responsible for respiration, reproduction and signalling).

Furthermore, the combination of optical tweezers with other techniques significantly enriches and strengthens both sides. So far, optical tweezers have been widely combined with microfluidic systems since a control over space and time as well as over the environment is provided. In addition, many optical techniques such as fluorescence microscopy (wide-field, confocal, TIRF and multiphoton microscopy) or Raman spectroscopy have also been implemented together with optical tweezers, achieving increased speed, sensitivity or resolution. Some other recent techniques with increasingly high resolutions are fluorescence resonance energy transfer, FRET, fluorescence lifetime imaging, FLIM, fluorescence after photobleaching, FRAP or stimulated emission depletion, STED; all of them currently partnering with optical trapping to some extent. Finally, the implementation of position detection systems such as FIONA (Fig. 7) for quantitative measurements of displacements and forces has also been reported [62].

5.a. Optical manipulation at the molecular scale

Until the advent of single-molecule techniques such as optical trapping, the study of biomolecular processes had been constrained to bulk experiments, which provided general averaged information of an entire population of molecules. Single molecule behaviour remained concealed and partially unknown. Optical tweezers and other similar techniques have revolutionized science across several disciplines making feasible experiments not previously possible. So far, hundreds of studies on single-molecule operating mechanisms, mechano-chemical energy conversions, conformational changes or mechanical properties of biomolecules have been performed.

Molecular motors are some of the most intensively studied proteins at the single-molecule level. The basic operating mechanism of these motor molecules consists of a chemical-mechanical energy conversion process. They play an essential role in cellular functions of immense significance, such as the replication of

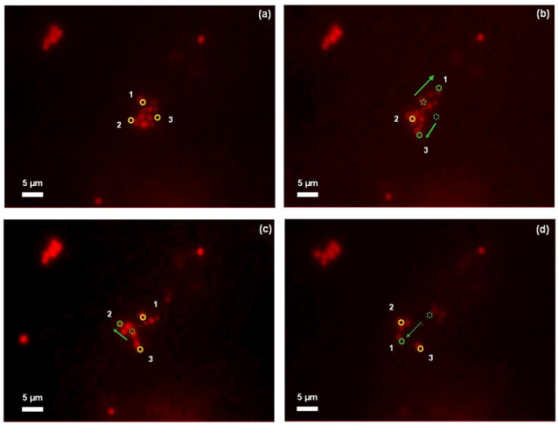

Fig. 7. **Manipulation of protein bodies with multiple optical traps in living tobacco cells (*Nicotiana Benthamiana*)**. Cereals, such as maize or rice, present a natural protein-storing mechanism that offers multiple advantages in plant development. This is essential to feed the embryo during the germination and seedling growth. Proteins are packaged inside 1-2 µm round shaped organelles called protein bodies (PBs). Presently, it is possible to artificially induce the formation of these structures in non-seed tissues, such as in the transgenic tobacco leaves shown in the image [83].

PBs are originated by vesiculation at the endoplasmatic reticulum (ER), a system of flattened cavities that serves as a transport network for molecules in cells. After 3-6 days post-infiltration (dpi), some PBs appear to be excreted from the ER into the cytosol. PBs move in a stop-go manner, i.e. alternating between periods of rapid-directed movement (velocity up to 6 µm/s) and periods of relatively diffusive or random motion. Furthermore, as the post-infiltration stage progresses, some PBs seem to be grouped as we can observe in the first image. At present, different questions about the morphology of this kind of structures are not well understood, such as whether groups of PBs are located at the same cavity (or lumen) of the endoplasmatic reticulum.

The sequence of images (extracted from a video) shows the real-time manipulation with three holographic optical traps (yellow circles) of a group constituted by at least 12 PBs (labelled with DsRed, 6 dpi). The green arrows indicate the displacement of the laser traps, which are conveniently controlled by means of our Holotrap application. From preliminary experiments, PBs seem to be covered by the ER membrane, suggesting that each PB is initially originated at a different endoplasmatic reticulum cavity and no fusion between PBs is possible.

DNA, RNA transcription, and the synthesis of proteins. At the cellular scale, they are responsible for processes such as cell division, vesicle trafficking, and endocytosis. At the tissue scale, they mediate the basic mechanisms of muscle contraction.

Several studies have been performed in order to **characterize the dynamics and kinetics** of molecular motors with optical tweezers. Linear motors that move along polymer tracks, such as cytoskeleton fibers or nucleic acids, are the target of many detailed assays. Among the former, extensive studies have been performed on different motors such as kinesin [2,58,84,85], myosin [4,61] or dynein [3,86] stepping along the cytoskeletal network in in vitro conditions and, quite recently, tracking of these motors in living cells, as well as some force measurements, has also become possible [14,87-90]. The latter basically refer to the study of the activity of processive enzymes such as RNA polymerases [5,41,91], DNA polymerases [92], helicases [93,94], topoisomerases [95] exonucleases [96] or translocases [97]. In addition, the study of other types of motors such as the portal motors responsible for viral packaging [98,99] has also been reported. Moreover, quantitative and qualitative characterization of the rotary motors found in flagellar motion, such as bacteria [100] or spermatozoa [101], has been extensively investigated. Furthermore, the operating mode of ribosomes in the synthesis of proteins has also been a topic under study [102].

This technique has also become very useful for the study of the mechanical properties of protein aggregates such as actin filaments [103,104] or microtubules [105,106], which constitute the cytoskeleton of the cell. These experiments have contributed to the understanding of diverse cellular phenomena such as muscle contraction, formation of cell shape, cell polarity, cell motion, cell division and organelle transport.

On the other hand, optical tweezers have been used to study the **mechanical properties** of several **biopolymers**. For instance, different properties of DNA and RNA mechanics [9,107-109], see Fig. 8, protein elasticity and conformational changes in folding/unfolding pathways [6,110,111], protein-protein [7,112] and DNA-protein [8] interactions have been and still are continuously explored. Moreover, the study of composite structures such as chromatin and chromosomes has provided a better understanding of the mechanical behaviour of its higher-order structure [113-115].

5.b. Optical manipulation at the cellular level

Optical tweezers have also been widely applied for several types of cellular studies, from single-cell to cell population studies.

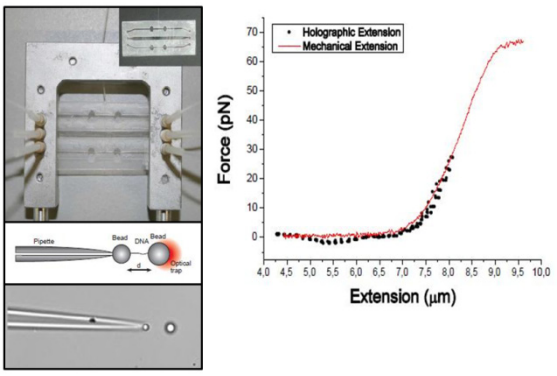

Fig. 8. **Study of DNA stretching with holographic optical tweezers**. A typical DNA pulling experiment registers the force-dependent stretching behaviour of the polymer. Here we show a preliminary experiment (video sequence) that compares a standard DNA stretching experiment with a holography-based version in order to determine its feasibility to reproduce similar results in terms of force, precision and sensitivity.

Both ends of the DNA strand are labelled with specific molecules, biotin and digoxigenin, and subsequently attached to two micro-beads that are coated with streptavidin and anti-digoxigenin. DNA manipulation requires a special fluidic chamber divided into three channels. The experiment is performed in the central channel, which is connected to a syringe with saline buffer that is used to wash the experimental area. Lateral channels are used to dispense the coated beads through independent paths. During the preparation, optical tweezers are used to trap each micro-bead coming from the channels and hold them until reaching the experimental area. One of the beads is strongly fixed by air suction with a micro-pipette, while the other is trapped with optical tweezers. Then, by increasing the distance between the two beads, the DNA strand is stretched.

Active manipulation of single cells such as cell confinement, transport, positioning, sorting, organizing or assembling is one of its most interesting applications. Optical tweezers have been used to immobilize, relocate, sort or assemble cells in a static or fluid flow environment with the purpose to perform cellular studies allowing for a real-time analysis of fluorescent, Raman, or morphological changes. Some of the main applications are cellular response studies to environmental stimuli [116-119]; identification, differentiation and maturation studies [120]; identification of different internal structures of the cell, cell sorting for distinction between living and dead cells or separation depending on their shape, size, refractive index and morphology [116,121-125]; relocation of cells to form new patterns or cell arrays [10,126-128] and simultaneous manipulation of arrayed cells [129-131]. Precise cell patterning is one of the main requisites for appropriate **tissue engineering**, which is one of the future prospects of optical tweezers.

Another interesting and powerful application of optical tweezers combined with UV, pulsed Nd:YAG or ultrashort pulsed fs laser microbeams is **cell nanosurgery**, in which the additional light source allows performing very precise cutting or controlled transient perforation with submicron resolution [11]. This novel microtool is known as optical scissors or scalpels. It has been employed to study the intracellular organelles [132], including chromosomes [11,133-135], the mitotic spindle, cytoskeletal filaments [136] and other subcellular components [137]. Moreover, such system has been used for the separation of individual cells from cell clusters [138]. The cell membrane may also be transiently permeabilized by applying CW or pulsed laser irradiation, allowing for **cell fusion** [139] (generation of hybrid cells) or molecular injection (opto-injection), leading to one of its most promising applications which is **cell transfection** [140]. Finally, quantitative studies of combinatorial chemistry with small volumes of reagents have also been performed [141,142].

Optical guiding with optical tweezers for the purpose of controlling neuronal cell growth is another suggested application [12,144,145]. Focused laser radiation on the leading edge of an active growth cone affects intracellular processes, such as the recruiting of actin monomers, which favours the cytoskeleton polymerization and induces growth towards the laser focus. This may have important implications for the formation of *in vitro* neuronal circuits and for the regeneration of damaged nerves *in vivo*.

The **mechanical characterization of cells** such as cell membrane properties (membrane tension or the cell response to defined load/stress) has become possible by means of stretching experiments. Modifications in the shape of a cell, such as bulging and ellipticity, can be used to infer the state of its cytoskeleton, which is an internal polymer structure capable of resisting external forces. This kind of studies has provided further insight into the understanding of the correlation between specific cellular structural changes and the onset

and progression of certain diseases. This is the case of red blood cells, whose modifications in their elastic and viscoelastic properties (shear modulus or relaxation time) represent a clear sign of infection, particularly from the malaria virus [146,147]. We find another important application in cancer studies, where the detection of changes in the deformability of cells can also be an alternative method to investigate the progression of this widespread disease [148]. For example, the optical stretcher [13], a close relative to optical traps, is designed to monitor cytoskeletal changes that may be indicative of cell malignancy, with unprecedented sensitivity. The system needs the presence of only 50 tumour cells in a sample for a reliable diagnosis, compared to the 10^4-10^5 required by traditional methods. Additionally, membrane mechanics has a direct effect on cell adhesion and reorientation [7, 149-151].

Finally, the **cells response to the interaction with laser light** has also been a topic that has received some attention, since it has an obvious impact on the validity of the results obtained in optical trapping experiments themselves. Ensuring cell viability and continued biological function after laser irradiation is a crucial point to guarantee meaningful results. A lot of studies have been performed with various cell types, including mammalian cells [152,153], Escherichia coli and Listeria bacteria [125,154-156], T cells, nerve cells, stem cells and pluricellular organisms such as Caenorhabditis elegans [157]. The cell damage has been evaluated by means of the analysis of several cell functions and reactions to damage such as the cloning efficiency, the ability to grow, motility, viability, apoptosis and stress response. Several parameters such as laser power (0-500mW), irradiation time (25-1200s) and wavelength (700-1064 nm) have been tested in order to determine a threshold value. The current conclusion is that for non-harming optical trapping of cells, continuous wave lasers in the NIR region, which experience a lower absorption in water and in biological tissues, should be used.

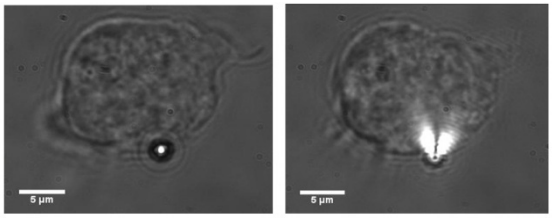

Fig. 9. **Study of the interaction between T Cells and Antigen Presenting Cells with holographic optical tweezers**. The possibility of measuring forces with optical tweezers enables us to use this physical magnitude as an indicator of the binding affinity in the immunological synapse [143]. Thus, a quantitative alternative to the standard binding kinematic studies is offered. In the experiment, we measure the rupture force of the link between the T Cell Receptor and Major Histocompatibility Complex (MHC) class II molecules complexed to cognate peptide ligands (pMHC). A pMHC-coated bead is brought in touch with the T cell membrane for a controlled period of time, enabling receptor recognition and formation of a physical contact. Strength of interaction under controlled conditions is next revealed by pulling the bead with optical tweezers.

6. Future prospects

A few decades have been sufficient for optical trapping to prove its immense potential, which will undoubtedly continue to expand and open new pathways for application. Here we summarize some of the prospects that we and others [20,23,25] envisage for the field. From a technological point of view, optical tweezers are undergoing a significant progress in two different fronts: the improvement of spatial/temporal resolution and accuracy for force measurements, and the hybridization with techniques for the simultaneous measurement of multiple parameters. The former developments will make possible the study of a much larger range of biological processes that occur at these length and time scales, a regime which has traditionally been quite inaccessible. Moreover, in some particular cases the elimination of noise sources will be essential to achieve even higher spatial resolution.

For example, improved resolution may make viable fast and inexpensive DNA sequencing by mechanically unzipping the double strand, pulling with an optical trap [158].

The combination of techniques provides the opportunity for additional readouts such as force and displacement along complementary axes, torque, and angle, or fluorescence position and orientation. Additionally, hybrid techniques

are expected to unleash the full arsenal of single-molecule fluorescence methods. As a result of this progress in optical tweezers instrumentation, many cellular processes involving conformational changes (proteins or nucleic acids) such as enzyme catalysis, cell signaling or ion channel gating can already be studied. In addition, direct observation and simultaneous measurement of distinct parameters of motion at the molecular scale (linear and rotatory motors for example) will be easily and accurately achieved. Furthermore, the combination of optical tweezers with microfluidic systems (lab-on-a-chip approach) is still a work in progress which will definitely allow a complete environmental control of molecular and cellular studies. Hence, the influence of pH, salt concentration, drugs or temperature can be investigated in real time.

The use of multiple traps has also high potential within simultaneous single-cell analysis. Automated workstations will easily provide improved statistics, and high-throughput manipulation for applications such as tissue engineering. Finally, improved methods for force measurements in arbitrary buffers [66, 79] will make possible the transition from simple *in vitro* experiments to explorations in more vivid biomimetic recreations of the cellular interior, eventually enabling the dream of full quantitative experiments inside living cells.

In conclusion, optical tweezers are a versatile and powerful tool in constant and continuous evolution which has certainly not reached its ceiling yet.

Acknowledgements

We are indebted to D. Ludevid and M. Joseph for providing the transformed samples of *Nicotiana Benthamiana* used in Fig. 7 as well as to T. Stratmann for providing the T-cells and coated beads used in Fig. 9. Also, F. Ritort kindly provided the DNA samples, coated microbeads and the microfluidic chamber used in Fig. 8.

Finally, we acknowledge the early contributions to this work by A. Carnicer, I. Juvells and S. Vallmitjana, and especially by M. S. Roth, E. Pleguezuelos and J. Andilla.

This work has been supported throughout the years by the Spanish Ministry of Science and Innovation, currently through project FIS2010-16104. Furthermore, J. Mas acknowledges an FPU grant from the Spanish Ministry of Education and A. Farré an FI grant from Generalitat de Catalunya.

